Available online at www.sciencedirect.com
ScienceDirect
Lithos 92 (2006) 83–104
LITHOS
www.elsevier.com/locate/lithos

A Hawaiian beginning for the Iceland plume: Modelling of reconnaissance data for olivine-hosted melt inclusions in Palaeogene picrite lavas from East Greenland

T.F.D. Nielsen [a,*], V.A. Turkov [b], I.P. Solovova [c], L.N. Kogarko [b], I.D. Ryabchikov [c]

[a] *Geological Survey of Denmark and Greenland, Øster Voldgade 10, DK-1350 Copenhagen K., Denmark*
[b] *Vernadsky Institute, 19 Kozygin Street, 119991 Moscow, Russia*
[c] *IGEM, Staromonetny Pereulok 35, 119017 Moscow, Russia*

Received 13 June 2005; accepted 27 March 2006
Available online 8 June 2006

Abstract

Compositions of parental and primary melts are modelled for olivine-hosted melt inclusions in three, Palaeogene, proto-Iceland plume picrite samples from East Greenland. The samples represent three stages in the magmatic evolution: (1) the early pre-spreading volcanics of the Lower Basalts, (2) the early plateau basalts in the Milne Land Formation and (3) the steady stage plateau basalt of the Geikie Plateau Formation. The observations suggest that the host lavas are variably mixed with melts and material from the wall rocks of the feeder system. Pressure estimates based on K_D between olivine and reconstructed melt composition suggests the melts to be trapped in their hosts during ascent from magma chambers near the base of the East Greenland crust. CaO/Al_2O_3 ratios suggest initiation of melting in the proto-Iceland plume at pressures up to 5–6 GPa and segregation depths mainly between 3 and 4 GPa. Early melts show marked similarities in major and trace elements with primary Hawaiian type melts. It is proposed that the continental separation in the North Atlantic was influenced by a pre-seafloor spreading rise of a "Hawaiian" type plume with a significant component of recycled basalt.

Keywords: Picrites; Palaeogene; East Greenland; Melt inclusions; Primary melts; Hawaiian type

1. Introduction

The up to ca. 8 km thick Palaeogene East Greenland plateau basalts formed prior to and during the continental break-up in the North Atlantic. Most of the plateau basalts are tholeiitic and quite evolved basaltic lavas (e.g., Brooks and Nielsen, 1982; Larsen et al., 1989; Fram and Lesher, 1997; Tegner et al., 1998a; Andreasen et al., 2004). The tholeiitic lavas are the result of magma pooling and fractionation in crustal magma chambers (e.g., Larsen et al., 1989; Andreasen et al., 2004). They give no direct insights in to the compositions and origins of the parental and primary magmas. Picritic lavas are not common in the East Greenland plateau basalt succession, but are potential sources for such information. The East Greenland picrite lavas and especially the earliest lavas are, however, often severely affected by burial metamorphism (e.g., Fram and Lesher, 1997; Hansen and Nielsen, 1999). In addition, the picrite lavas contain a spectrum of olivine morphologies, e.g., Nielsen et al. (1981). Although the

* Corresponding author.
E-mail address: tfn@geus.dk (T.F.D. Nielsen).

0024-4937/$ - see front matter © 2006 Elsevier B.V. All rights reserved.
doi:10.1016/j.lithos.2006.03.038

bulk rock compositions of the picrite lavas and dykes would be closer to those of primary, mantle-derived melts, they too may be the result of magma pooling and magma chamber processes.

Melt inclusions in olivine phenocrysts and xenocrysts are a source for information on the compositions of primary magmas (e.g., Gurenko and Chaussidon, 1995; Gurenko et al., 1996; Kamenetsky et al., 1998; Kent et al., 2002; Yaxley et al., 2004; Sobolev et al., 2005). The interpretation of melt inclusion data is, however, often difficult as their compositions vary widely compared to the often well constrained volcanic suites (e.g., Danyushevsky et al., 2004). This reconnaissance study presents analyses and interpretations for melt inclusions from three picrite samples from the East Greenland flood basalt province. The aim is to identify deep and primary, enriched, plume components in the earliest stages of the proto-Iceland plume and to evaluated the potential for a comprehensive study of primary melts in the earliest stages of the proto-Iceland plume from compositions of olivine-hosted melt inclusions.

The data for this study were acquired in the framework of INTAS project 95-953 in 1996-97 and reported in Brooks and Ryabchikov (1998). The present author provided the samples and the background information for the study. Some of the data was presented in Turkov et al. (1998) and Ryabchikov et al. (1998), but only in the form of extended abstracts.

2. The investigated materials

2.1. The Lower Basalts

The up to ca. 1.5 km thick Lower Basalts is a succession of early lavas exposed in the Kangerlussusaq region (e.g. Nielsen et al., 1981; Fram and Lesher, 1997; Hansen and Nielsen, 1999). They are deposited in a continental rift environment and are at their base interbedded with sediments accumulated since early Cretaceous (see, e.g., Nielsen et al., 1981; Larsen et al., 1999; Peate et al., 2003). The Lower Basalts are subdivided into the Vandfaldsdalen Formation and the Mikis Formation (Nielsen et al., 1981) and separated from the overlying regional plateau basalt formations by the Hængefjeldet Formation. The Hængefjeldet Formation is dominated by subaerial and waterlain basaltic tuffs (Nielsen et al., 1981; Peate et al., 2003). The Vandfaldsdalen Formation is a regional succession of lavas deposited in the continental rift system. They are subaerial to the south-west, near the supposed centre of the Kangerlussuaq triple junction and the supposed centre of impact of the proto-Iceland plume under the coast of East Greenland (e.g., Brooks, 1973). They form hyaloclastites and pillow lavas in the deeper, more easterly parts of the rift environment. The overlying, subaerial Mikis Formation appears to form a large, ca. 1 km thick, shield like structure within the rift system (Nielsen et al., 1981).

The picrites of the Lower Basalts are represented by sample GGU 361026 (Table 1) from the lowest 10 m thick picrite flow in the Lower Vandfaldsdalen Formation. The flow is exposed in the eastern wall of Sødalen (Fig. 1; Nielsen et al., 1981; Fram and Lesher, 1997). The investigated sample was collected from a large block on the valley floor. The reason is that the large, broken-up blocks offer much fresher material than can be collected in situ. The picrite sample is massive, dense and contains numeral up to 2 mm large, fresh, olivine phenocrysts and small olivine-clinopyroxene intergrowths in a very fine-grained black matrix composed of clinopyroxene, Fe–Ti oxides, plagioclase and altered olivine and glass. The olivine phenocrysts and the intergrowths are generally fresh and evenly distributed in the flow (see Nielsen et al., 1981 for illustrations and further details). No post-extrusion accumulation of olivine is suggested and the sample is believed to represent the phenocryst-bearing magma.

As other picrite flows from the Lower Basalts, sample GGU 361026 contains three morphologies of olivines: (1) euhedral olivines zoned from 89% to 87% forsterite that appear to be in equilibrium with the bulk composition of the lava (Mg# 0.74; Table 1); (2) embayed and resorbed olivines (up to Fo_{91}) that do not appear to

Table 1
Whole rock compositions

Sample #	361026	404017	40648
Formation	Lower Basalts	Milne land formation	Geikie P. Formation time-equivalent
	Lava	Lava	Dyke
Mg#	0.738	0.744	0.779
SiO_2	45.41	45.72	44.61
TiO_2	1.83	1.33	1.58
Al_2O_3	9.00	8.93	7.07
Fe_2O_3	1.60	1.70	1.89
FeO	9.80	9.95	10.34
MnO	0.19	0.17	0.15
MgO	17.73	18.77	23.80
CaO	8.19	7.10	7.58
Na_2O	1.41	1.21	0.72
K_2O	0.15	0.30	0.24
P_2O_5	0.19	0.16	0.12
Volatiles[a]	2.65	4.34	2.33
Total	98.15	99.68	100.43

XRF analyses by Geological Survey of Denmark and Greenland.
[a] Loss in ignition.

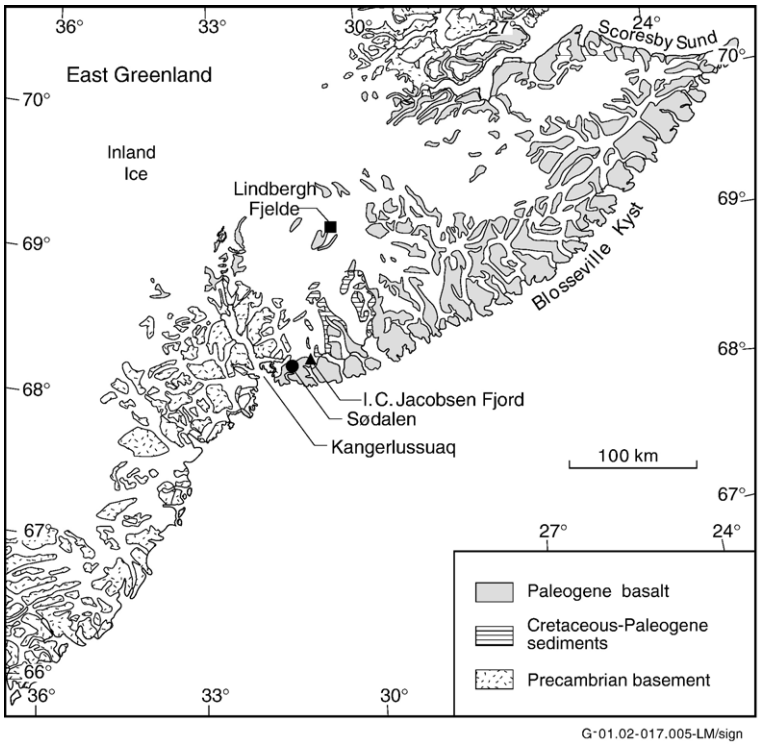

Fig. 1. Sampling sites for the three investigated samples.

be in equilibrium with the carrying melt; and (3) olivines ($Fo_{86–85}$ rimmed down to Fo_{81}) in aggregates with grass-green, chrome-diopside (e.g., Nielsen et al., 1981). The clinopyroxenes have low Al_2O_3 contents and show no high-pressure affinities (Nielsen et al., 1981; Brooks and Nielsen, 1982). They are suggested to be fragments of cumulates formed in magma chambers in or near the base of the East Greenland crust or from the walls of the feeder system. Olivine compositions from sample 361026 are shown in Table 2.

The bulk rock composition (Table 1; Fig. 2A) is a typical, tholeiitic picrite from the Lower Basalts with 1.83 wt.% TiO_2 and 17.73 wt.% MgO. The reader is referred to Nielsen et al. (1981), Brooks and Nielsen

Table 2
Compositions of host olivines

Sample	361026	361026	361026	361026	361026	404017	404017	404017	404017	40648	40648	40648
Grain #	1	2	2	3	4	1	2	3	5	5	8	9
SiO_2	41.14	40.82	40.71	41.03	40.65	39.21	39.60	39.54	39.58	40.02	38.53	38.66
TiO_2	0.13	b.d.	b.d.	b.d.	b.d.	0.12	b.d.	b.d.	b.d.	b.d.	b.d.	b.d.
Al_2O_3	b.d.	b.d.	b.d.	b.d.	b.d.	b.d.	b.d.	b.d.	b.d.	b.d.	b.d.	b.d.
Cr_2O_3	0.15	0.10	0.15	0.12	0.06	0.09	0.10	0.07	0.12	b.d.	0.07	b.d.
FeO	9.31	10.79	10.12	9.37	14.33	13.29	14.46	12.99	13.14	15.02	16.56	16.61
MnO	0.21	n.a.	0.21	0.14	0.18	n.a.	n.a.	n.a.	n.a.	n.a.	n.a.	n.a.
MgO	48.60	48.07	47.97	49.38	44.92	45.30	44.85	45.53	45.78	44.30	40.97	42.15
NiO	0.45	0.38	0.47	0.48	0.42	0.32	0.37	0.29	0.41	0.30	0.24	0.29
CaO	0.35	0.31	0.15	0.21	0.38	0.22	0.32	0.27	0.17	0.33	0.18	0.31
Na_2O	b.d.	0.01	b.d.	0.03	b.d.	b.d.	0.03	0.04	b.d.	b.d.	0.03	0.01
Sum	100.34	100.48	99.78	100.76	100.94	98.55	99.73	98.80	99.20	99.97	96.58	98.03
Fo %	90.29	88.81	89.41	90.38	84.82	85.86	84.68	86.20	86.13	84.01	81.51	81.89

b.d.: below detection.
n.a.: not analysed.

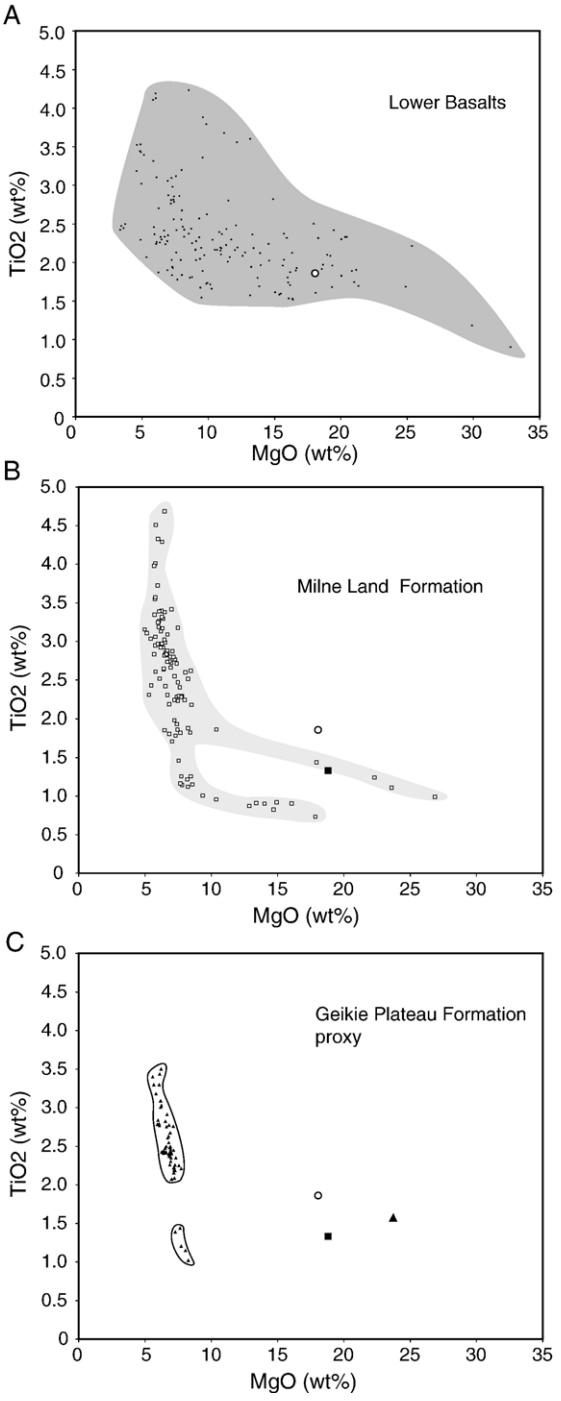

Fig. 2. Compositions of host rocks (Table 1) and formations. (A) The Lower Basalts in East Greenland (Hansen and Nielsen, 1999). The large circle is the here studied picrite sample (GGU 361026); (B) Milne Land Formation (Tegner et al., 1998a). The large filled square is the here studied picrite sample (GGU 404017). The large circle is the studied Lower Basalts picrite and (C) the Geikie Plateau Formation (Tegner et al., 1998a). The large filled triangle is the here studied picrite sample (GM 40648). The circle and the filled square are the studied Lower Basalts and Milne Land Formation picrites (see (A) and (B)). All analyses recalculated to 100% volatile-free.

(1982), Fram and Lesher (1997) and Hansen and Nielsen (1999) for a more comprehensive description of the mineralogy, chemistry and evolution of the Lower Basalts.

2.2. Milne Land Formation

The Milne Land Formation is the first voluminous and regional plateau basalt Formation in East Greenland (Larsen et al., 1989). It can be traced across the entire East Greenland Province and across the North Atlantic to the Faeroe Islands (Pedersen et al., 1997). The sample from the Milne Land Formation originates from a sequence of picrite flows in the lower part of the Formation in Lindbergh Fjelde, some 70 km inland (Fig. 1). The sample was collected 1.5 m up from the base of a 7 m thick olivine-rich flow that shows no significant variation in the concentration of olivine (L.M. Larsen, pers. com., 2005). The sample is suggested to represent the phenocryst-bearing magma as extruded.

The 1–2 mm size olivine phenocrysts form a quite homogenous group with $Fo_{85–86}$ (Table 2). They are not resorbed and appear morphologically to be in equilibrium with the carrying melt. The equilibrium olivines suggest the melt to have a Mg# of ca. 68. The bulk rock is with a Mg# of 0.74 (Table 1) believed to be cumulative. The matrix is very fine-grained and composed of clinopyroxene, plagioclase, Fe–Ti oxides and altered olivine and glass. The composition of the picrite differs from the previous picrite in having lower TiO_2 and FeO (Table 1 and Fig. 2B) and it belongs to a small subgroup of TiO_2-rich picrites within the formation.

2.3. Geikie Plateau Formation

The up to 1 km thick Geikie Plateau Formation is one of the most voluminous and regional formations in the East Greenland Plateau Basalts (Larsen et al., 1989; Pedersen et al., 1997; Andreasen et al., 2004). It is composed of more uniform FeTi-basalts and represents two major cycles of extrusion from large magma chambers. The geochemical variation is quite systematic (e.g., Andreasen et al., 2004; Tegner et al., 1998a). Andreasen et al. (2004) suggest that a steady state had been established and that the magmas equilibrated and homogenised in large magma chambers, where assimilation of crustal material, fractionation and crystallisation took place simultaneously.

No picrite lavas occur in the Geikie Plateau Formation. The picrite sample taken to be a time-equivalent to the Geikie Plateau Formation originates

from a dyke (GM 40648). The dyke intrudes the Mikis formation of the Lower Basalts 150 m above sea level above the major "Sill Point" picrite sills, at the head of Jacobsen Fjord (Fig. 1; Nielsen et al., 1981). It belongs to a suite of radial dykes correlated in time to the Skaergaard intrusion (Nielsen, 1978; Brooks and Nielsen, 1978). The Skaergaard intrusion is on the basis of bulk chemical composition, age and pressure of crystallisation correlated in time to the Geikie Plateau Formation (Nielsen, 2004; Andreasen et al., 2004; Tegner, pers. com., 2005). These relations suggest the selected dyke to be contemporaneous with the Geikie Plateau Formation.

The dyke is up to 15 m wide and appears quite homogenous with little variation in the proportion of olivine. As for the lava samples, it is believed to be representative for the phenocryst-bearing magma that was emplaced into the dyke. Sample (GGU 40648) is unaltered and contains abundant fresh olivine (Fo_{84-81}) phenocrysts (Table 2). They are up to 3 mm in size, euhedral and appear to be in equilibrium with the carrying melt. The bulk rock MgO is high (23.8 wt.% MgO, Mg#=0.78; Table 1; Fig. 2C). The olivine compositions suggest a melt Mg# around 0.64 and the sample is olivine cumulative. The groundmass is composed of fine-grained clinopyroxene, plagioclase, FeTi-oxides and altered glass.

3. The melt inclusions

Olivine-hosted melt inclusions are rare and they are in many cases not well preserved, especially in the sample from the Lower Basalts (Brooks and Ryabchikov, 1998). Inclusions near cracks and alteration products have been discarded in the study. The studied melt inclusions are 5–50 μm in size with most inclusions between 5 and 25 μm. They are commonly partially crystallised (some glass is preserved) and some contain a little fluid. Their rounded shapes suggest that the trapped melts have crystallised olivine along their walls. No inclusions with the shape of negative crystals have been observed. The daughter minerals include orthopyroxene, spinel, ilmenite and amphibole, in addition to olivine (Brooks and Ryabchikov, 1998).

3.1. Analytical methods

The aim of this reconnaissance study is to use the data in Brooks and Ryabchikov (1998) for the modelling of the compositions of melts as they were trapped in their olivine hosts. The obtained compositions are then used as the basis for the modelling of early, enriched, primary melts of the proto-Iceland plume. Most of the inclusions are partially crystallised and re-heating and quenching is required before the composition of the melt can be determined. The techniques and methods are described in Sobolev (1996). Melt inclusions wholly enclosed in glassy, translucent olivine were heated at 1 bar until all daughter minerals, except for an unknown proportion of olivine along the margins of the inclusions, were melted to form a homogeneous melt (V. Turkov, Vernadsky Institute, Moscow, pers. comm., 1996). A rapid quench produced glass inclusions. Care was taken not to overheat the inclusions and risk decrepitation. Some of the inclusion may have been underheated, whereas others may have been overheated. Only homogenous glasses were analysed. Homogenisation temperatures are not quoted in Brooks and Ryabchikov (1998) for the studied samples, but for one Lower Basalts picrite (same suite as sample GGU 361026). The homogenisation temperature was 1240 °C for an inclusion melt with 9.01 wt.% MgO, Mg#=0.63 and K_D=0.34.

The inclusions were exposed by polishing and subsequently analysed using a JEOL Superprobe at the Department of Geology, University of Copenhagen, using a WDS standard setting (Larsen et al., 2003). Normal operating conditions were 15 kV accelerating voltage and 15 nA beam current, and 20 s counting time. The detection limits are by the laboratory quoted to be 0.01%. The compositions of the analysed inclusions are shown in Table 3.

Trace element analyses were provided by A. Sobolev and acquired at Institute of Microelectronics, Russian Academy of Sciences (Jaroslavl', Russia) using an IMS-4f ion microprobe. The methods, detection limits, etc. are described in detail in Sobolev (1996). The provided trace element data (Electronic appendix 1) are averages of several compositionally similar analyses within individual grains. Note should be taken that only a limited number of melt inclusions were sufficiently large for the acquisition of ion probe analyses.

4. Compositions of experimental and natural glass inclusions

All analytical data for the experimental and natural glass inclusions used in this study (Table 3) originates from the reconnaissance studies in Brooks and Ryabchikov (1998). The glasses were not analysed for P_2O_5 and in some cases for MnO and the NiO concentrations were in some cases below detection. In addition, it should be mentioned that the alkali content may not be entirely stable due to volatilisation during analysis at

Table 3
Compositions of homogenised melt inclusions

Sample #	GGU	GGU	GGU	GGU	GGU	GGU	GGU	GGU	GGU	GGU	GGU	GGU	GGU	GGU	GGU	GGU	GGU	GGU	GGU	GGU	GGU	GGU	GGU
	361026	361026	361026	361026	361026	361026	361026	361026	361026	361026	361026	361026	361026	361026	361026	404017	404017	404017	404017	404017	404017	404017	404017
Olivine grain #	1	1	1	2	2	2	2	2	2	3	3	4	4	4	4	1	1	1	1	2	2	2	3
Analysis #	1	2	3	4	5	6	7	8	9	10	11	12	13	14	15	1	2	3	4	5	6	7	8
Composition																							
SiO_2	49.21	49.65	48.86	47.79	47.24	52.37	51.71	54.94	55.58	60.82	60.01	49.85	48.50	48.86	49.83	46.51	48.37	46.92	46.89	47.77	47.04	47.58	46.42
TiO_2	2.72	2.44	2.60	3.10	2.70	1.53	1.83	1.52	1.67	0.92	1.08	2.42	2.07	2.45	2.67	1.62	1.48	1.40	1.63	1.57	1.45	1.42	1.30
Al_2O_3	11.13	11.70	10.94	11.05	10.52	7.05	6.73	5.61	5.63	4.69	4.80	12.45	12.40	12.47	12.45	10.22	11.19	10.73	11.60	9.28	9.15	9.01	9.66
FeO	11.67	10.99	11.46	14.94	15.37	17.28	17.03	16.70	16.49	9.67	10.06	12.16	11.76	10.97	12.44	12.03	11.48	10.94	10.55	13.75	14.51	14.37	16.75
MgO	13.50	13.83	13.56	9.42	9.93	10.94	10.83	8.44	8.59	18.62	18.21	9.67	9.65	9.25	9.57	13.58	13.15	14.49	11.99	13.73	15.98	14.89	8.99
NiO	0.03	0.08	0.09	b.d.	0.05	0.09	b.d.	b.d.	0.06	0.15	0.08	0.01	0.06	b.d.	b.d.	0.13	b.d.	0.09	0.08	0.10	0.05	0.05	b.d.
MnO	n.a.	n.a.	0.27	n.a.	0.22	0.25	0.13	0.25	n.a.	0.22	n.a.	0.22	n.a.	0.26	n.a.	n.a.	n.a.	n.a.	n.a	n.a.	n.a.	n.a.	n.a.
CaO	9.58	9.56	9.77	10.20	10.38	9.18	8.84	10.38	9.58	3.72	4.13	10.82	11.07	10.89	10.82	8.30	8.87	7.67	8.23	9.14	8.75	8.87	7.61
Na_2O	1.37	1.36	1.20	2.08	1.91	0.62	0.65	0.63	0.62	0.70	0.59	0.84	2.36	2.10	2.32	2.08	2.01	2.31	2.45	1.75	1.48	1.62	2.01
K_2O	0.07	0.08	0.14	0.34	0.13	0.13	0.23	0.08	0.10	0.06	0.12	0.30	0.35	0.34	0.34	0.14	0.27	0.22	0.23	0.13	0.19	0.08	0.11
Cr_2O_3	0.25	0.23	0.18	0.23	0.23	0.39	0.39	0.29	0.25	0.13	0.15	0.03	0.03	0.04	b.d.	0.06	0.13	0.03	b.d.	0.44	0.45	0.42	0.31
Sum	99.68	100.07	99.22	99.35	98.88	100.06	98.59	99.06	98.79	99.83	99.36	98.93	98.41	97.77	100.60	94.83	97.10	94.94	93.79	97.84	99.24	98.50	93.38
Calc. Fe_2O_3[a]	1.54	1.45	1.51	1.97	2.03	2.28	2.25	2.21	2.18	1.28	1.33	1.61	1.55	1.45	1.64	1.59	1.52	1.45	1.39	1.82	1.92	1.90	2.21
Calculated FeO	10.28	9.68	10.10	13.16	13.54	15.23	15.01	14.71	14.53	8.52	8.86	10.71	10.36	9.67	10.96	10.60	10.12	9.64	9.30	12.12	12.78	12.66	14.76
Mg#	0.701	0.718	0.705	0.560	0.566	0.561	0.563	0.505	0.513	0.796	0.785	0.617	0.624	0.630	0.609	0.695	0.698	0.728	0.697	0.669	0.690	0.677	0.520
Equilibrium olivine[b]	87.64	87.17	86.64	78.38	78.52	78.17	78.25	74.39	74.97	91.23	90.72	81.58	82.05	82.44	81.07	86.28	86.45	88.06	86.36	84.76	85.98	85.23	74.64
Observed olivine	90.29	90.29	90.29	88.81	88.81	89.41	89.41	89.41	89.41	90.38	90.38	84.82	84.82	84.82	84.82	85.86	85.86	85.86	85.86	84.68	84.68	84.68	86.20

Sample #	GGU	GGU	GGU	GGU	GGU	GGU	GGU	GGU	GGU	GM	GM	GM	GM	GM	GM	GM	GM	GM	GM	GM
	404017	404017	404017	404017	404017	404017	404017	404017	404017	40648	40648	40648	40648	40648	40648	40648	40648	40648	40648	40648
Olivine grain #	3	3	3	3	5	5	5	5	5	9	8	8	8	8	8	8	5	5	5	9
Analysis #	9	10	11	12	13	14	15	16	17	1	4	5	6	7	8	9	10	11	12	13
Composition																				
SiO_2	46.57	46.12	47.22	46.70	49.29	52.44	49.10	49.14	48.95	45.38	44.03	44.52	44.80	43.88	46.32	41.65	44.69	46.87	46.7	46.49
TiO_2	1.28	0.98	1.08	1.03	1.93	1.92	1.25	1.48	1.50	1.83	2.09	2.14	2.15	1.65	2.15	1.27	1.88	1.97	2.07	1.97
Al_2O_3	9.56	9.69	10.09	9.92	11.19	11.37	10.54	11.19	10.90	9.47	9.86	10.00	10.62	8.77	10.66	7.50	11.34	10.62	11.22	11.22
FeO	17.66	15.76	17.84	16.58	12.27	12.50	11.04	10.20	10.67	14.42	16.15	17.29	15.53	16.69	17.79	13.55	14.73	12.47	12.81	14.56
MgO	9.52	13.50	9.27	9.77	13.10	13.33	15.02	14.76	15.12	14.08	8.57	7.16	6.75	13.03	7.06	19.50	8.69	8.31	7.48	9.87
NiO	0.01	0.08	0.06	0.04	0.03	0.01	0.10	0.06	0.08	0.06	b.d.	b.d.	0.13	0.06	b.d.	0.09	0.03	0.05	0.01	0
MnO	n.a.	n.a.	n.a.	n.a.	n.a.	n.a.	n.a.	n.a.	n.a.	n.a.	n.a.	n.a.	n.a.	n.a.	n.a.	n.a.	0	0	0	0
CaO	7.57	6.53	7.40	7.30	8.20	8.97	8.10	8.03	8.34	9.16	10.12	10.68	10.72	8.62	11.14	6.73	10.09	11.04	10.75	10.13
Na_2O	2.01	2.14	2.13	2.29	2.53	2.51	2.14	2.09	2.17	1.86	1.91	1.82	2.13	1.64	1.74	1.43	2.06	1.68	1.83	1.91
K_2O	0.17	0.28	0.12	0.11	0.22	0.24	0.30	0.41	0.43	0.17	0.19	0.20	0.28	0.12	0.27	b.d.	0.18	0.28	0.1	0.28
Cr_2O_3	0.31	0.34	0.41	0.34	0.20	0.23	0.19	0.19	0.16	0.06	0.06	0.03	0.10	0.09	0.04	0.06	1.26	0.13	0.16	0.13
Sum	94.89	95.63	95.86	94.30	99.12	103.69	97.93	97.68	98.46	96.68	93.19	94.07	93.41	94.77	97.40	91.96	95.14	93.58	93.3	96.75
Calc. Fe_2O_3[a]	2.33	2.08	2.36	2.19	1.62	1.65	1.46	1.35	1.41	1.90	2.13	2.28	2.05	2.20	2.35	1.79	1.95	1.65	1.69	1.92
Calculated FeO	15.56	13.89	15.72	14.61	10.81	11.01	9.73	8.99	9.40	12.71	14.23	15.23	13.68	14.71	15.67	11.94	12.98	10.99	11.29	12.83
Mg#	0.522	0.634	0.512	0.544	0.683	0.683	0.733	0.745	0.741	0.664	0.518	0.456	0.468	0.612	0.445	0.744	0.544	0.574	0.541	0.578
Equilibrium olivine[b]	74.72	82.45	74.02	76.36	85.41	85.40	88.18	88.81	88.6	84.88	75.31	70.42	71.42	81.78	69.52	89.22	76.66	78.77	76.48	79.58
Observed olivine	86.20	86.20	86.20	86.20	86.13	86.13	86.13	86.13	86.13	81.89	81.51	81.51	81.51	81.51	81.51	81.51	84.01	84.01	84.01	81.89

b.d.: below detection.

n.a.: not analysed.

[a] Fe_2O_3/FeO after Brooks (1976).

[b] Using K_D estimated from Fig. 2 in Herzberg and O'Hara (1998).

15 kV and 15 nA. The Fe_2O_3/FeO ratio has been set at 0.15 as a first approximation (Brooks, 1976). The compositions are all tholeiitic and range from basaltic to picritic, except for two silica-rich composition from natural glass inclusions (Table 3a, 361026, anal. 10 and 11). The picritic to basaltic composition corroborates with the fields of East Greenland volcanics (Fig. 3).

4.1. Modelling of the trapped compositions

The experimental glass compositions do, however, not represent the trapped melts or primary melts. The melt inclusions have mostly been insufficiently heated to achieve equilibrium between melt and host due to the risk of decrepitation. Olivine should accordingly be added (or subtracted in the case of overheating) to obtain equilibrium between the host and the originally trapped melt. It is assumed that the melt was in equilibrium with its olivine host at the time of entrapment. Providing a correlation between the Mg# of the olivine and the Mg# of the melt can be established it is possible to add or subtract host olivine until equilibrium between host and trapped liquid is obtained. Olivine compositions in equilibrium with the observed melts (Fig. 4) have been calculated in accordance with Herzberg and O'Hara (2002, Fig. 2; $K_{D,\,FeO/MgO}^{Ol/L} = 0.381 - 0.790/MgO + 1.039/MgO^2$). The Mg# of melt in equilibrium with a host olivine can be estimated in Fig. 4 and the composition of the trapped melt can then be calculated by subtraction or addition of host olivine until the Mg# of the equilibrium

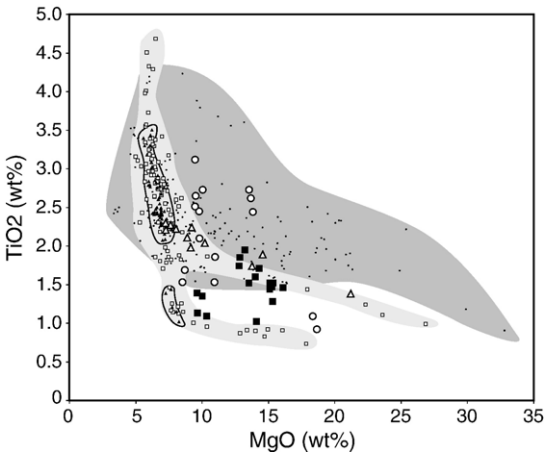

Fig. 3. Composition of glasses of homogenised melt inclusions (Table 3; Brooks and Ryabchikov, 1998). Large circles: melts from the Lower Basalts (GGU 361026), filled squares: melts from the Milne Land Formation (GGU 404017) and large triangles: melts from the Geikie Plateau Formation time-equivalent (GM 40648). Compositional fields lavas from the Lower Basalts, Milne Land and Geikie Plateau Formations from Fig. 2A–C.

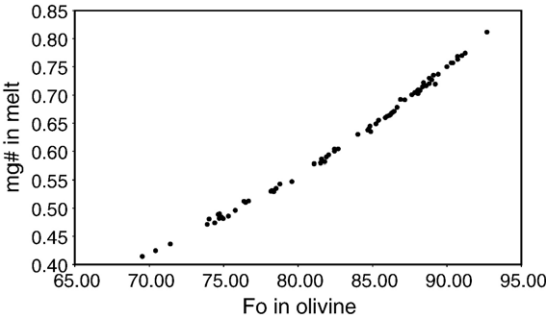

Fig. 4. Correlation between Mg# of calculated equilibrium olivine and homogenised melt compositions (Table 3) using the K_D equation of Herzberg and O'Hara (2002). The figure is used for the estimate of the K_D for a melt in equilibrium with a given olivine composition. See text for explanation.

melt (as dictated by the host olivine) has been reached. The reason for this approach is that the $K_{D,\,FeO/MgO}^{Ol/L}$ is not a constant. Tables 4a, 4b and 4c show the compositions of the trapped melts after equilibration to their host olivines and the amount of added (or subtracted) olivine and the Fo % of host olivine (from Table 2).

The major element composition of the trapped melts fall well inside the entire spectrum of East Greenland whole rock compositions (Fig. 5). They divide into three groups. One group with >20 wt.% MgO represents wall reaction products (see below). The compositions with <20 wt.% MgO divide into a high- to medium-TiO_2 group and a low-TiO_2 group. Both of these melt types are present in the studied sample from the Lower Basalts as well as in the Milne Land Formation sample, despite the fact that no bulk rock composition from the Lower Basalts come close to the TiO_2-poor compositions. The melts from the Geikie Plateau Formation time-equivalent belong to a suite of compositions between medium- and high-TiO_2 compositions similar to those found in the Lower Basalts and the Milne Land Formation (Fig. 5). With few exceptions, the experimentally equilibrated compositions from the Lower Basalts and the Milne Land Formation fall within the fields of their respective bulk rock compositions (Fig. 5).

No Fe diffusion between trapped melt and olivine host is assumed in the above calculation, despite the fact that 10–40% Fe is generally lost to the olivine host (see, e.g., Danyushevsky et al., 2000; Sobolev et al., 2000). A Fe loss due to diffusion would have lowered the FeO(total) content in the melts in Table 3. A correction for the loss of Fe can be made by comparing melt inclusion FeO(total) with the compositions of the lavas from which the melt inclusions originate. The significant spread in FeO(total) contents in the East Greenland lavas (e.g., Nielsen et al.,

Table 4a
Trapped melts in GGU 361026

Sample #	GGU	GGU	GGU	GGU	GGU	GGU	GGU	GGU	GGU	GGU	GGU	GGU	GGU	GGU	GGU
	361026	361026	361026	361026	361026	361026	361026	361026	361026	361026	361026	361026	361026	361026	361026
Analysis #	1	2	3	4	5	6	7	8	9	10	11	12	13	14	15
Comment[a]						WR react.	WR react.	WR react.	WR react.	Incong. m.	Incong. m.				
Host Fo %	90.29	90.29	90.29	88.81	88.81	89.41	89.41	89.41	89.41	90.38	90.38	84.82	84.82	84.82	84.82
Added olivine[a]	13.92	9.59	12.82	33.65	34.12	40.45	40.31	46.2	44.82	0.00	0.00	4.22	3.09	2.06	5.3
SiO_2	48.77	48.26	48.31	46.13	45.94	49.02	49.10	50.82	51.40	60.92	60.40	49.98	48.92	49.77	48.97
TiO_2	2.23	2.41	2.34	2.33	2.04	1.09	1.32	1.05	1.16	0.92	1.09	2.35	2.04	2.46	2.52
Al_2O_3	10.65	9.78	9.77	8.30	7.93	5.02	4.86	3.87	3.93	4.70	4.83	12.07	12.20	12.50	11.73
Cr_2O_3	0.22	0.24	0.18	0.20	0.20	0.32	0.33	0.25	0.22	0.13	0.15	0.03	0.03	0.04	b.d.
Fe_2O_3	1.32	1.35	1.35	1.48	1.53	1.62	1.63	1.52	1.52	1.28	1.34	1.56	1.53	1.45	1.55
FeO	9.62	10.17	10.07	12.59	12.93	13.75	13.76	13.36	13.27	8.53	8.92	10.97	10.62	9.97	11.04
MnO	0.20	0.20	0.26	0.20	0.22	0.24	0.15	0.24	0.20	0.22	n.a.	0.22	0.20	0.26	0.20
MgO	16.82	17.78	17.62	19.10	19.63	21.63	21.64	21.02	20.87	18.65	18.33	11.18	10.83	10.17	11.25
NiO	0.11	0.08	0.13	0.10	0.13	0.20	0.14	0.16	0.19	0.15	0.08	0.03	0.07	0.02	0.03
CaO	8.73	8.46	8.77	7.74	7.90	6.58	6.43	7.21	6.73	3.73	4.16	10.51	10.90	10.92	10.21
Na_2O	1.24	1.20	1.07	1.57	1.44	0.44	0.47	0.43	0.43	0.70	0.59	0.81	2.32	2.10	2.19
K_2O	0.07	0.06	0.13	0.26	0.10	0.09	0.17	0.06	0.07	0.06	0.12	0.29	0.34	0.34	0.32
Sum	99.98	99.99	100.00	100.00	99.99	100.00	100.00	99.99	99.99	99.99	100.01	100.00	100.00	100.00	100.01
Mg#[b]	0.757	0.757	0.757	0.730	0.730	0.737	0.737	0.737	0.737	0.796	0.785	0.645	0.645	0.645	0.645
CaO/Al_2O_3	0.820	0.865	0.898	0.933	0.996	1.311	1.323	1.863	1.712	0.794	0.861	0.871	0.893	0.874	0.870
FeO (total)	10.81	11.38	11.28	13.92	14.31	15.21	15.23	14.73	14.64	9.68	10.13	12.37	12.00	11.27	12.43
Fe_2O_3/FeO[c]	0.137	0.133	0.134	0.118	0.118	0.118	0.118	0.114	0.115	0.150	0.150	0.142	0.144	0.145	0.140

WR react.: wall rock reaction product.
Incong. m.: incongruent melt.
b.d.: below detection.
n.a.: not analysed.
[a] Host olivine added to give melt Mg# corresponding to host olivine Mg# (Fig. 4).
[b] Melt Mg# as suggested by host olivine (Fig. 4).
[c] Fe_2O_3/FeO after olivine correction.

Table 4b
Trapped melts in GGU 404017

Sample #	GGU	GGU	GGU	GGU	GGU	GGU	GGU	GGU	GGU	GGU	GGU	GGU	GGU	GGU	GGU	GGU	GGU
	404017	404017	404017	404017	404017	404017	404017	404017	404017	404017	404017	404017	404017	404017	404017	404017	404017
Analysis #	1	2	3	4	5	6	7	8	9	10	11	12	13	15	15	16	17
Comment[a]								WR react.	WR react.	WR react.	WR react.	WR react.	WR react.	Contam.	Contam.	Contam.	Contam.
Host Fo %	85.86	85.86	85.86	85.86	84.68	84.68	84.68	86.2	86.2	86.2	86.2	86.2	86.13	86.13	86.13	86.13	86.13
Added olivine[a]	−6.85	−7.02	−13.43	−6.4	−5.83	−10.98	−7.85	−3.8	−3.9	−3.58	−3.9	−3.75	−3.57	−13.74	−13.74	−15.6	−15.15
SiO_2	49.62	50.44	50.81	50.58	49.29	48.24	48.94	47.65	47.10	47.62	47.18	47.71	49.99	51.66	51.70	52.12	51.37
TiO_2	1.82	1.63	1.68	1.84	1.70	1.64	1.56	1.11	1.07	0.96	0.88	0.89	2.02	1.48	1.48	1.79	1.79
Al_2O_3	11.55	12.37	13.03	13.18	10.05	10.34	9.91	8.23	7.97	9.49	8.25	8.61	11.68	12.45	12.46	13.55	13.02
Cr_2O_3	0.06	0.14	0.02	b.d.	0.47	0.50	0.45	0.28	0.27	0.34	0.35	0.31	0.20	0.21	0.21	0.21	0.17
Fe_2O_3	1.79	1.68	1.75	1.58	1.97	2.17	2.09	1.89	1.94	2.04	1.93	1.90	1.69	1.72	0.95	1.63	1.68
FeO	10.98	10.16	9.62	9.65	12.23	12.66	12.69	15.23	15.69	14.41	15.67	15.04	10.80	9.39	10.10	8.44	8.87
MnO	0.21	0.21	0.21	0.21	0.20	0.20	0.20	0.21	0.21	0.21	0.21	0.21	0.20	0.20	0.20	0.20	0.20
MgO	11.97	11.07	10.47	10.51	12.09	12.52	12.55	16.97	17.48	16.05	17.45	16.75	11.97	10.41	10.41	9.35	9.84
NiO	0.12	b.d.	0.06	0.07	0.09	0.01	0.02	0.06	0.07	0.10	0.11	0.09	0.02	0.05	0.05	b.d.	0.02
CaO	9.36	9.79	9.28	9.33	9.88	9.85	9.73	6.54	6.36	6.41	6.11	6.38	8.56	9.54	9.55	9.69	9.93
Na_2O	2.35	2.22	2.80	2.78	1.89	1.67	1.78	1.72	1.68	2.10	1.75	1.99	2.64	2.53	2.53	2.53	2.59
K_2O	0.16	0.30	0.27	0.26	0.14	0.21	0.09	0.11	0.16	0.28	0.11	0.11	0.23	0.35	0.35	0.50	0.51
Sum	99.99	100.01	100.00	99.99	100.00	100.01	100.01	100.00	100.00	100.01	100.00	99.99	100.00	99.99	99.99	100.01	99.99
Mg#[b]	0.660	0.660	0.660	0.660	0.638	0.638	0.638	0.665	0.665	0.665	0.665	0.665	0.664	0.664	0.647	0.664	0.664
CaO/Al_2O_3	0.810	0.791	0.712	0.708	0.983	0.953	0.982	0.795	0.798	0.675	0.741	0.741	0.733	0.766	0.766	0.715	0.763
FeO (total)	12.59	11.67	11.19	11.07	14.00	14.61	14.57	16.93	17.44	16.25	17.41	16.75	12.32	10.94	10.95	9.91	10.38
Fe_2O_3/FeO[c]	0.163	0.165	0.182	0.164	0.161	0.171	0.165	0.124	0.124	0.142	0.123	0.126	0.156	0.183	0.094	0.193	0.189

WR react.: wall rock reaction product.
Contam.: contaminated with crustal melt.
b.d.: below detection.
[a] Host olivine added to give melt Mg# corresponding to host olivine Mg# (Fig. 4).
[b] Melt Mg# as suggested by host olivine (Fig. 4).
[c] Fe_2O_3/FeO after olivine correction.

Table 4c
Trapped melts in GM 40648

Sample #	GM	GM	GM	GM	GM	GM	GM	GM	GM	GM	GM	GM
	40648	40648	40648	40648	40648	40648	40648	40648	40648	40648	40648	40648
Analysis #	1	4	5	6	7	8	9	10	10	11	12	13
Host Fo %	81.89	81.51	81.51	81.51	81.51	81.51	81.51	84.01	84.01	84.01	84.01	81.89
Added olivine [a]	−13.48	9.05	16.95	14.16	−5.91	17.92	−38.25	12.85	12.85	7.67	11.62	1.72
Added chromite								−2.1				
SiO_2	48.01	46.53	46.15	46.86	46.61	46.28	48.53	46.10	47.08	49.28	48.92	47.76
TiO_2	2.18	2.05	1.94	2.01	1.85	1.87	2.23	1.75	1.75	1.95	1.98	2.00
Al_2O_3	11.30	9.68	9.07	9.94	9.81	9.26	13.18	10.54	10.59	10.52	10.75	11.37
Cr_2O_3	0.07	0.06	0.04	0.10	0.10	0.05	0.06	1.17	0.05	0.13	0.15	0.13
Fe_2O_3	2.27	2.09	2.07	1.92	2.47	2.04	3.15	1.81	1.69	1.63	1.62	1.95
FeO	12.52	15.39	16.30	14.93	15.38	16.22	10.38	13.73	13.69	11.92	12.34	13.28
MnO	0.21	0.21	0.21	0.21	0.21	0.21	0.22	0.21	0.20	0.21	0.21	0.21
MgO	10.11	11.93	12.63	11.57	11.92	12.57	8.05	13.12	13.13	11.39	11.79	10.72
NiO	0.03	0.03	0.05	0.15	0.05	0.05	0.01	0.06	0.06	0.07	0.04	0.11
CaO	10.88	9.95	9.71	10.06	9.63	9.71	11.71	9.42	9.62	10.96	10.33	10.27
Na_2O	2.22	1.88	1.66	2.00	1.83	1.52	2.49	1.92	1.96	1.67	1.76	1.93
K_2O	0.20	0.19	0.18	0.26	0.13	0.23	b.d.	0.17	0.17	0.28	0.10	0.28
Sum	100.00	99.99	100.01	100.01	99.99	100.01	100.01	100.00	99.99	100.01	99.99	100.01
Mg# [b]	0.590	0.580	0.580	0.580	0.580	0.580	0.580	0.630	0.631	0.630	0.630	0.590
CaO/Al_2O_3	0.960	1.030	1.070	1.010	0.980	1.050	0.890	0.890	0.910	1.040	0.960	0.900
FeO (total)	14.56	17.27	18.16	16.66	17.6	18.06	13.21	15.36	15.21	13.39	13.8	15.03
Fe_2O_3/FeO [c]	0.181	0.136	0.127	0.129	0.161	0.126	0.303	0.132	0.123	0.137	0.131	0.147

WR react.: wall rock reaction product.
b.d.: below detection.
[a] Host olivine added to give melt Mg# corresponding to host olivine Mg# (Fig. 4).
[b] Melt Mg# as suggested by host olivine (Fig. 4).
[c] Fe_2O_3/FeO after olivine correction.

1981; Larsen et al., 1989; Fram and Lesher, 1997; Hansen and Nielsen, 1999) prohibits such a Fe correction in accordance with, e.g., Danyushevsky et al. (2000) and Sobolev et al. (2000). Some uncertainty remains, but the fact that most of the modelled parental compositions fall in the field of their respective formations and resemble host rock compositions suggests that Fe diffusion was limited. It is also noted that many of experimental glasses have high FeO(total) and that a loss of 40% FeO would lead to extreme compositions with 14–21 wt.% FeO(total) at Mg#'s of 0.77–0.58.

4.2. Reaction melts

The compositions of the trapped liquids represent compositions of melts in the feeder system of the volcanics. Some trapped melts may represent the ascending magma and others may be products of reaction between ascending magma and wall rocks, or melts from upper mantle domains (e.g., Sobolev et al., 2000; Danyushevsky et al., 2004; Yaxley et al., 2004). All of these melts contribute to the bulk compositions of the lavas and the dyke, though in very different proportions. Some may be strongly enriched in specific components, which would lead to distortion of, e.g., trace element ratios and isotopic compositions. In other words, bulk rock compositions of the lavas and the dyke cannot a priori be assumed to represent the products of simple melting scenarios.

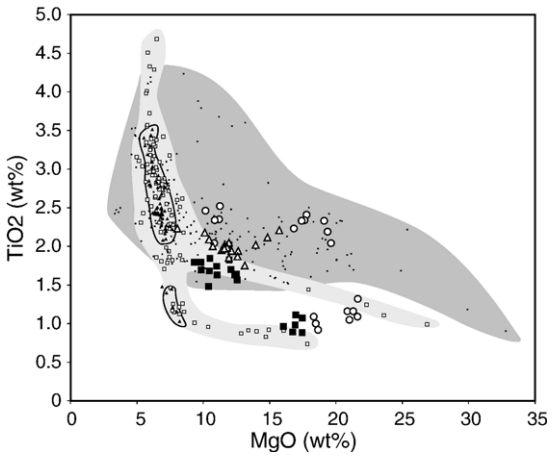

Fig. 5. Compositions of trapped melts after equilibration with host olivine (Tables 4a, 4b and 4c). See Fig. 2 for further explanation.

Some of the compositions stand out in Fig. 5 and in Tables 4a, 4b and 4c. Compositions 361026/10–11 from natural glass inclusions (Brooks and Ryabchikov, 1998) have high Mg#'s, are low in TiO_2 and have high SiO_2 (ca. 60 wt.% SiO_2; Table 4a). A mass balance mix composed of 65% of this melt and 35% of the host olivine has the composition of an orthopyroxene (Table 5). The calculation suggests a nearly stoichiometric mineral composition. It is suggested the high-silica melt is the product of incongruent melting of orthopyroxene included in the olivine grain. The composition resembles orthopyroxene from an eclogitic source (Table 5) (Ramsay and Thompkins, 1994). It cannot be excluded that the melting of orthopyroxene has been facilitated by a minor amount of melt trapped alongside the orthopyroxene. The olivine host has a Fo content of 90.3%. Olivines from the Lower Basalts with >90% forsterite are generally resorbed (Nielsen et al., 1981) and the olivine and its orthopyroxene inclusion are suggested to be xenocrystic. They could represent wall rock material entrained and heated in ascending, hot, picrite magma.

Table 5
Mass balance model for incongruent melt

	Average 361026 10–11	Olivine host	Modelled orthopyroxene 65% melt+35% olivine host	Eclogitic orthopyroxene [a]
SiO_2	60.52	40.72	53.59	53.23
TiO_2	1.00	b.d.	0.65	0.36
Al_2O_3	4.75	b.d.	3.09	4.93
Cr_2O_3	0.14	0.12	0.13	0.20
Fe_2O_3	n.a.	n.a.	n.a.	n.a.
FeO	10.15	9.30	9.85	10.63
MnO	0.21	0.14	0.19	0.15
MgO	18.45	49.01	29.15	29.52
NiO	0.12	0.48	0.24	n.d.
CaO	3.93	0.21	2.63	0.81
Na_2O	0.65	0.03	0.43	0.15
K_2O	0.09	b.d.	0.06	0.03
Sum	100.01	100.00	100.01	100.00
Mg#	0.764	0.904	0.841	0.832
Cations				
Si			1.904	1.872
Ti			0.017	0.009
Al			0.129	0.305
Cr			0.000	0.005
Fe^{3+}			0.000	0.042
Fe^{2+}			0.293	0.270
Mn			0.006	0.004
Mg			1.540	1.547
Ni			0.007	n.d.
Ca			0.100	0.030
Na			0.030	0.100
K			0.003	0.001
			0.000	0.000
Si+Al(IV)			2.00	2.00
Others+ remaining Al			2.03	1.99

b.d.: below detection.
n.a.: not analysed.
[a] Bronzite, eclogite nodule, Sale Lake, Hawaii (Kuno, 1969).

A second abnormal type of inclusion is characteristically low in TiO_2, Na_2O, Al_2O_3 and CaO and high in FeO(total) and Cr (Tables 4a, 361026/4b, and 4b, 404017/8–12)). It is suggested to be produced by the addition of melts or material from a depleted, chromite-bearing, paragenesis, i.e., material crystallised on the walls of the feeder system or alternatively from a depleted upper mantle peridotite. Such melts compose most of the compositions in the low-TiO_2 group (Fig. 5). Similar melts are described from melt inclusions in the Baffin Bay picrites (Yaxley et al., 2004).

A third abnormal type is silica-enriched basaltic melts (e.g., Table 4b: 404017/15–17 and 4c: 40648/9). Besides SiO_2, they appear to have elevated Al_2O_3 that nay be caused probably by crustal contamination. Attempts to calculate the equilibrium olivine (see below) fail. The isotopic and elemental variations show that crustally contaminated composition occurs throughout the flood basalt succession (e.g., Holm, 1988; Larsen et al., 1989; Fram and Lesher, 1997; Hansen and Nielsen, 1999). Such contaminated melts are also reported from the Baffin Bay picrites (Yaxley et al., 2004) and will not be discussed further.

4.3. Average compositions of the trapped melts

Several melt inclusions have been analysed in many of the studied olivine grains. In many cases, adjacent inclusions in single grains have very similar major element compositions. The compositions have been averaged to give a representative composition for the melt in which the olivine grain crystallised (Table 6). The average trace element compositions provided by A. V Sobolev (see above and Electronic appendix 2) relate to these compositions. They are in Table 6 corrected for the amount of olivine used for the calibration between melt inclusion and host (see Tables 4a, 4b and 4c). The averages in Table 6 are the starting compositions for the back-calculation to melts in equilibrium with mantle.

5. Back-calculation to primary melts

5.1. Temperature and pressure of entrapment.

The trapped melts may not be primary melts, as the melts may have experienced fractional crystallisation

Table 6
Compositions of trapped melts

Sample #	GGU	GGU	GGU	GGU	GGU	GGU	GGU	GGU	GGU	GM	GM	GM	GM	GM
	361026	361026	361026	361026	361026	404017	404017	404017	404017	40648	40648	40648	40648	40648
Analysis #	1–3	4–5	6–9	10–11	12–15	1–4	5–7	8–12	13	1	4–8	10	11–12	13
	average	average	average	average	average	average	average	average			average		average	
Host Fo %	90.29	88.81	89.41	90.38	84.82	85.86	84.68	86.20	86.13	81.89	81.51	84.01	84.01	81.89
Added olivine	10.78	25.31	30.02	0.00	3.53	−8.41	−8.22	−3.79	−3.57	−13.48	8.90	13.45	8.77	1.72
Added chromite												−2.1		
Calc. olivine [a]	90.30	88.75	89.36	void	84.75	85.82	84.44	86.15	86.10	81.47	81.46	83.96	83.99	81.56
P (kbar) [a]	8.5	14.4	0.8	void	1.2	0.4	0.001	1.5	1.6	0.001	0.7	5.1	0.8	0.001
T (°C) [a]	1433.7	1515.8	1442.6	void	1276.8	1285.8	1300	1395.5	1315.5	1255.6	1302.8	1351.5	1288.8	1270.5
Major elements (wt.%)														
SiO_2	48.45	46.03	50.06	60.59	49.41	50.36	48.82	47.41	49.99	48.03	46.46	47.08	49.08	47.82
TiO_2	2.33	2.19	1.16	1.00	2.34	1.74	1.63	0.98	2.02	2.18	1.94	1.75	1.97	2.00
Al_2O_3	10.07	8.12	4.42	4.76	12.13	12.53	10.10	8.51	11.68	11.30	9.55	10.59	10.64	11.38
Cr_2O_3	0.21	0.20	0.28	0.14	0.03	0.06	0.47	0.31	0.20	0.07	0.07	0.05	0.14	0.13
Fe_2O_3	1.47	1.51	2.09	1.31	1.15	1.59	2.08	2.90	1.80	1.70	2.56	1.69	1.47	1.51
FeO	9.83	12.76	13.06	8.72	10.99	10.20	12.53	14.34	10.70	13.07	15.24	13.69	12.28	13.69
MnO	0.22	0.21	0.21	0.22	0.22	0.21	0.20	0.21	0.20	0.21	0.21	0.20	0.21	0.21
MgO	17.41	19.36	21.28	18.47	10.86	11.01	12.39	16.90	11.97	10.11	12.12	13.13	11.59	10.73
NiO	0.11	0.12	0.17	0.11	0.04	0.06	0.04	0.09	0.02	0.03	0.07	0.06	0.06	0.02
CaO	8.65	7.82	6.74	3.94	10.64	9.44	9.82	6.36	8.56	10.88	9.81	9.62	10.65	10.28
Na_2O	1.17	1.51	0.44	0.64	1.86	2.54	1.78	1.85	2.64	2.22	1.78	1.96	1.72	1.94
K_2O	0.09	0.18	0.10	0.09	0.32	0.25	0.15	0.15	0.23	0.20	0.20	0.17	0.19	0.28
Sum	100.00	100.01	100.01	99.99	99.99	99.99	100.01	100.01	100.01	100.00	100.01	99.99	100.00	99.99
Mg#	0.757	0.73	0.744	0.791	0.638	0.658	0.638	0.677	0.666	0.58	0.586	0.631	0.627	0.583
FeO (total)	11.16	14.12	14.94	9.90	12.02	11.63	14.40	16.95	12.32	14.60	17.54	15.21	13.60	15.05
Fe_2O_3/FeO	0.14	0.12	0.16	0.15	0.11	0.16	0.17	0.20	0.17	0.13	0.17	0.12	0.12	0.11
Log fO_2 [a]	−4.40	−4.42	−4.23	void	−6.91	−6.11	−5.80	−4.44	−5.69	−6.90	−5.87	−5.93	−5.93	−6.99
CaO/Al_2O_3	0.859	0.963	1.525	0.828	0.877	0.753	0.972	0.747	0.733	0.963	1.027	0.908	1.001	0.903
Trace elements corrected for added olivine (ppm)														
Ba	36.91	n.a.	15.16	16.76	36.19	108.82	108.13	66.51	76.83	12.54	20.33	n.a.	26.47	10.67
Th	0.32	n.a.	0.03	0.24	0.54	0.36	0.24	0.17	0.29	0.03	0.25	n.a.	0.18	0.03
Nb	6.10	n.a.	1.42	5.00	6.63	7.87	7.81	5.22	7.75	2.05	4.85	n.a.	4.45	1.74
La	6.73	n.a.	0.97	4.78	7.13	8.13	8.10	4.89	7.15	2.08	3.86	n.a.	3.60	1.77
Sr	208.15	n.a.	89.26	122.00	253.39	267.08	274.99	170.46	253.27	52.64	128.36	n.a.	122.63	44.77
Ce	18.72	n.a.	3.15	12.99	21.57	23.12	20.45	12.93	19.09	5.74	10.54	n.a.	10.84	4.89
Nd	14.22	n.a.	2.92	9.07	16.49	15.91	14.77	9.04	15.52	3.80	8.13	n.a.	7.88	3.23
Zr	100.20	n.a.	24.23	63.72	114.26	109.34	97.09	67.14	108.71	28.11	61.36	n.a.	57.83	23.91
Sm	4.08	n.a.	0.78	2.41	4.91	5.34	4.15	2.62	4.31	1.24	2.12	n.a.	2.70	1.05
Eu cor.	1.26	n.a.	0.25	0.76	1.57	1.19	1.67	0.83	1.46	0.61	0.76	n.a.	0.74	0.52
Dy	3.76	n.a.	0.70	2.10	4.26	3.99	3.72	1.94	2.97	0.99	1.95	n.a.	2.13	0.85
Y	20.07	n.a.	4.01	11.98	23.31	19.85	18.78	9.93	16.72	4.39	11.76	n.a.	11.84	3.74
Er	1.81	n.a.	0.49	1.02	2.41	1.73	2.16	1.07	1.57	0.55	1.27	n.a.	1.22	0.47
Yb	1.57	n.a.	0.32	1.13	2.00	1.65	1.73	0.87	1.22	0.39	0.99	n.a.	1.09	0.33

n.a.: not analysed.
[a] After Larsen and Pedersen (2000).

before entrapment. The compositions have to be back-calculated to a likely mantle equilibrium, i.e., equilibrium olivine. Larsen and Pedersen (2000) developed a stepwise back-calculation of liquid compositions following the principles described in Albarède (1992) and Sobolev and Nikogosian (1994). Each step represents the addition of 0.5% olivine. The method is described in detail in the electronic supplements to Larsen and Pedersen (2000). The method is based on the algorithms of Ford et al. (1983), Kilinc et al. (1983) and Sack et al. (1980). Calculated liquidus olivine will only be stoichiometric

at a specific P and T at a given $K_{D,\ FeO/MgO}^{Ol/L}$ (see Larsen and Pedersen, 2000 for further details). NiO and MnO have in the calculations been set to a minimum of 0.01 wt.% (detection limit) and 0.20 wt. %, respectively, if no concentration is reported in Brooks and Ryabchikov (Table 6).

The calculation of Larsen and Pedersen (2000) (see example in Electronic appendix 2) has been developed for the back-calculation of the compositions of volcanic glasses quenched at 1 bar. It is, however, not known at which P and T the East Greenland inclusions were originally trapped. A starting P and T has to be established before the back-calculation can be performed. One, although rather rough method, is to estimate the pressure from the $K_{D,\ FeO/MgO}^{Ol/L}$. The model of Larsen and Pedersen (2000) can be calibrated using a K_D calculated from the algorithm of Herzberg and O'Hara (2002) ($K_{D,\ FeO/MgO}^{Ol/L} = 0.381 - 0.790/MgO + 0.039/MgO^2$, with a statistical error of 0.019 at 1 standard deviation). The Herzberg and O'Hara algorithm is based on the MgO content in coexisting experimental liquids and olivines, and appears (see below) to be rather robust. P and T and the Fe_2O_3/FeO ratio are adjusted in increments until the K_D in the Larsen and Pedersen model is equal to the K_D calculated according to Herzberg and O'Hara and the composition of the host olivine is reproduced.

The uncertainty on the calculation is significant (Electronic appendix 3). A change of ±0.01 on the K_D value leads to errors on P of ±2.5 kbar, ±10 °C and ±0.6 log units for fO_2. Although the error seems forbidding, the calculations lead to reasonable results. For two of the Hawaiian compositions (Table 8, columns 2 and 6), the error on temperature is about 9 °C, equivalent to an error on the pressure of approximately 2 kbar assuming a gradient of 46 °C/GPa. Compositions in columns 3 and 4 (Table 8) give a much higher error (30–40 °C), which seems to be a reflection of the of a low estimate (ΔT=40 °C) for the temperature of the source regions of Mauna Kea and Kilauea melts in Sobolev et al. (2005). It is questioned if it is reasonable to assume a drop in temperature of 40 °C at a depth of ca. 90 km for a lateral distance of only 30 km in the source regions of the Hawaiian plume. It is here estimated that the error on the P is in the order of ±2.5 kbar when the K_D of Herzberg and O'Hara (2002) is used as a constraint in the calculations of Larsen and Pedersen (2000).

The first step in the back-calculation to primary compositions in equilibrium with source is an iterative adjustments of the P in steps of 0.2 kbar starting at 1 bar and T until the calculated olivine is stoichiometric and the K_D calculated according to Larsen and Pedersen (2000) is identical to the K_D calculated as suggested by Herzberg and O'Hara (2002). The Fe_2O_3/FeO is not fixed and the fO_2 is not buffered in the calculation.

The second step is the correction of Fe_2O_3/FeO and re-adjustment of P and T to obtain a calculated composition of liquidus olivine as close as possible to the composition of the observed host. The calculations give approximations to the P, T and log fO_2 at the time the melt inclusion was trapped. Log fO_2 values are in this study generally −6.2±0.5 for melts with ca. 12 wt. % MgO and −4.8±0.4 for melts with ca. 20 wt.% MgO. The P, T, log fO_2 and the calculated compositions of liquidus olivine for the melt inclusions are shown in Table 6.

The estimated pressures and temperatures of entrapment (Table 6) suggest that the investigated melt inclusions were trapped in olivines crystallised during the ascent of the melts. Pressures between 1 bar and 14.8 kbar and temperatures between 1255 and 1515 °C are calculated. Note should be taken that no clear correlation exists between P and T. Melts suggested to be wall rock reaction products may equilibrate at high T, but low P, probably because they were entrained in ascending, hot, picrite magma (Table 6; e.g., 361026/6–9 entrained in, e.g., 361026/1–3 or 4–5).

5.2. Constraints for the modelling of primary melts

A primary melt is a melt in equilibrium with its mantle source. Addition of equilibrium olivine to the compositions of the trapped melts in Table 6 will

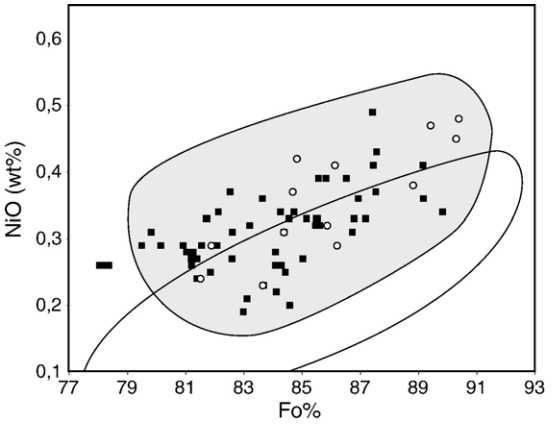

Fig. 6. Ni content in olivines from the Lower Basalts in East Greenland. Filled squares: compositions from Hansen (1993) and circles: compositions of host olivines from Brooks and Ryabchikov (1998, Table 2 in this work). Grey field: olivines from Hawaii and lower field phenocrysts from ocean ridge basalts (copied from Sobolev et al., 2005).

Table 7
Primary melts

Formation stage	Lower Basalts				Milne Land Formation					Geikie Plateau Formation			
	Pre-spreading magmatism				Early, non-steady, plateau basalt stage					Steady state plateau basalt stage			
	1	2	3	4	5	6	7	8	9	10	11	12	13
Inclusions #	361026/1-3	361026/4-5	361026/6-9	361026/12-15	404017/1-4	404017/5-7	404017/8-12	404017/13	40648/1	40648/4-8	40648/10	40648/11-12	40648/13
Comment	WR react.						WR react.						
T (°C) [a]	1433.70	1515.80	1442.60	1461.90	1423.70	1490.30	1471.60	1490.9	1512.00	1468.55	1517.90	1457.80	1521.65
P (kbar) [a]	8.50	14.40	0.80	12.00	8.20	10.70	6.00	11.40	14.80	10.50	14.50	10.40	14.60
Olivine added	0.00	0.00	0.00	18.17	13.53	20.59	10.44	18.98	24.47	17.76	18.58	17.34	25.23
Equilibrium olivine (Fo %)	90.30	88.75	89.36	89.05	89.00	89.00	88.00	90.03	88.01	86.00	88.03	88.01	88.02
Major elements (wt.%)													
SiO_2	48.45	46.03	50.06	47.76	49.02	47.08	46.67	48.20	46.08	45.28	45.81	47.52	45.86
TiO_2	2.33	2.19	1.16	1.92	1.51	1.29	0.88	1.64	1.65	1.60	1.42	1.63	1.50
Al_2O_3	10.07	8.12	4.42	9.93	10.84	8.02	7.62	9.46	8.53	7.85	8.62	8.80	8.51
Cr_2O_3	0.21	0.20	0.28	0.04	0.06	0.39	0.29	0.18	0.08	0.07	0.06	0.13	0.12
Fe_2O_3	1.47	1.40	2.09	0.94	1.38	1.65	2.60	1.46	1.28	2.11	1.37	1.22	1.13
FeO	9.83	12.86	13.06	11.22	10.43	12.47	14.12	10.79	13.27	15.21	13.57	12.51	13.74
MnO	0.22	0.21	0.21	0.22	0.21	0.20	0.21	0.20	0.21	0.21	0.20	0.21	0.21
MgO	17.41	19.36	21.28	17.33	15.85	19.41	19.99	18.68	18.69	17.81	19.21	17.45	19.42
NiO	0.11	0.12	0.17	0.11	0.11	0.11	0.12	0.10	0.12	0.12	0.12	0.11	0.110
CaO	8.65	7.82	6.74	8.76	8.20	7.86	5.73	6.99	8.29	8.12	7.89	8.86	7.77
Na_2O	1.17	1.51	0.44	1.52	2.20	1.41	1.66	2.14	1.68	1.46	1.60	1.42	1.45
K_2O	0.09	0.18	0.10	0.26	0.22	0.12	0.13	0.19	0.15	0.16	0.14	0.16	0.21
Sum	100.01	100.00	100.01	100.00	100.03	100.01	100.02	100.03	100.03	100.00	100.01	100.02	100.03
Mg#	0.759	0.728	0.745	0.734	0.732	0.736	0.717	0.757	0.716	0.677	0.717	0.714	0.717
Ni (ppm)	864	943	1336	864	864	864	943	786	943	943	943	864	864
Log fO_2 [a]	−4.40	−4.42	−4.22	−5.40	−5.02	−4.36	−3.89	−4.38	−4.91	−4.59	−4.73	−5.27	−5.08
FeO(total)	11.15	14.12	14.94	12.07	11.67	13.95	16.46	12.10	14.42	17.11	14.80	13.61	14.76
CaO/Al_2O_3	0.859	0.963	1.525	0.882	0.756	0.980	0.752	0.739	0.972	1.034	0.915	1.007	0.913
Segregation P (kbar) [b]	32	40	void	34	25	41	25	25	40	47	38	32	38
Trace elements (ppm)													
Ni	864	943	1336	841	849	880	967	770	904	943	967	896	880
Ba	36.91	n.a.	16.76	30.63	95.85	89.67	60.22	64.58	10.08	17.26	n.a.	22.56	8.52
Th	0.32	n.a.	0.24	0.46	0.32	0.2	0.15	0.24	0.03	0.21	n.a.	0.16	0.02
Nb	6.1	n.a.	5	5.61	6.93	6.48	4.72	6.51	1.64	4.12	n.a.	3.79	1.39
K	749.32	n.a.	747.09	2306.94	1836.11	1050.02	1328.11	1591.72	1387.46	1424.06	n.a.	1300.78	1889.79
La	6.73	n.a.	4.78	6.03	7.16	6.71	4.42	6.01	1.67	3.28	n.a.	3.07	1.41
Sr	208.15	n.a.	122	214.42	235.25	228.04	154.35	212.87	42.29	109	n.a.	104.5	35.75
Ce	18.72	n.a.	12.99	18.25	20.37	16.96	11.71	16.05	4.62	8.95	n.a.	9.24	3.9
Nd	14.22	n.a.	9.07	13.95	14.01	12.25	8.19	13.05	3.06	6.9	n.a.	6.71	2.58
Zr	100.2	n.a.	63.72	96.69	96.31	80.51	60.8	91.37	22.58	52.11	n.a.	49.28	19.09
Sm	4.08	n.a.	2.41	4.15	4.7	3.44	2.37	3.63	0.99	1.8	n.a.	2.3	0.84
Eu cor.	1.26	n.a.	0.76	1.33	1.05	1.38	0.75	1.23	0.49	0.65	n.a.	0.63	0.42
Dy	3.76	n.a.	2.1	3.6	3.51	3.08	1.76	2.49	0.8	1.65	n.a.	1.82	0.68
Y	20.07	n.a.	11.98	19.72	17.48	15.58	8.99	14.05	3.53	9.99	n.a.	10.09	2.98
Er	1.81	n.a.	1.02	2.04	1.52	1.79	0.97	1.32	0.45	1.08	n.a.	1.04	0.38
Yb	1.57	n.a.	1.13	1.69	1.45	1.44	0.79	1.03	0.32	0.84	n.a.	0.93	0.27

n.a.: not analysed.

[a] Calculated as suggested by Larsen and Pedersen (2000) using constraint on KD from Herzberg and O'Hara (2002). See text for details.

[b] Segregation depth estimated from CaO/Al_2O_3 ratio and Al_2O_3 concentration according to Herzberg and Zhang (1996). See Fig. 9 and text for details.

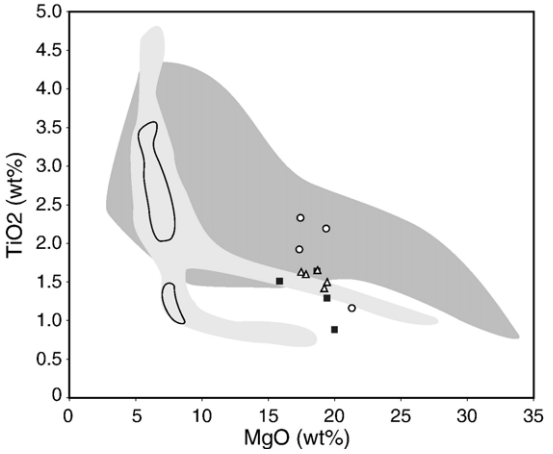

Fig. 7. Average compositions for primary melts (Table 7). Circles: Lower Basalts, filled squares: Milne Land Formation and open triangles: Geikie Plateau Formation time-equivalent. Compositional field for Lower Basalts (grey), Milne Land Formation (light grey) and Geikie Plateau Formation (black lines) from Fig. 2A–C.

increase the Mg# and Ni content of the liquids and the equilibrium olivines will become more and more forsterite and Ni-rich. The crucial question is: How much equilibrium olivine should be added? Korenaga and Kelemen (2000) questioned the back-calculation of North Atlantic magmas to equilibrium olivines in the $Fo_{88–91}$ range (Fram and Lesher, 1997) on the basis of the Ni content. Based on a average Ni content of 3500 ppm in source rock olivines, Korenaga and Kelemen calculated a maximum Ni in primary liquids of <500 ppm. They suggest that the North Atlantic mantle contains a proportion of recycled oceanic crust and that this component was responsible for low Mg#.

Liquids with higher Ni contents can be obtained, e.g., from a heterogeneous, eclogite-bearing, mantle source (Sobolev et al., 2005). It seems likely the Ni content of primary liquids could be well above the upper limit of 500 ppm (Korenaga and Kelemen, 2000) if melt fractions from a heterogeneous source were pooled.

A high Ni content in Hawaiian liquidus olivines relative to the compositions from common seafloor basalts supports this view (Sobolev et al., 2005). As in the shield building stages of Hawaii, the picrites of the Lower Basalts of East Greenland (Fig. 6; data from sources in footnotes) have NiO contents elevated relative to average mantle peridotites, abyssal peridotites and ocean-ridge basalts. The Ni contents appear to be distinctly higher than in, e.g., Iceland, West Greenland and oceanic olivines (see Sobolev et al., 2005 for a compilation).

Following Sobolev et al. (2005), the compositions of the East Greenland melt inclusions have been calculated back to an upper limit of ca. 1000 ppm Ni. Approximation to a Ni/MgO ratio of 40–50 is chosen to allow a comparison with primary melts from Hawaii, as described in Sobolev et al. (2005). The back-calculated melt compositions (Table 7) are in equilibrium with olivines down to Fo_{86} in agreement with the suggestions of Korenaga and Kelemen (2000) and have, with the exception of a wall rock reaction product, Ni/MgO ratios of 40–50. Calculation to forsterite contents of 91% leads to unreasonable Ni contents well above 1000 ppm.

5.3. The modelled compositions of primary melts

The modelled major element compositions and the normalised trace element compositions are shown in Table 7 and Figs. 7 and 8. The trace element compositions have been corrected for the dilution caused by the addition of olivine. The calculated major element compositions fall in the high-MgO range of the known volcanic East Greenland suites (Fig. 7). It is believed that the here calculated melts are approximations to the composition of primary melts in their source regions. The melts divide into three groups:

(a) Group A includes trace element-rich compositions of two melt inclusions from the Lower Basalts and

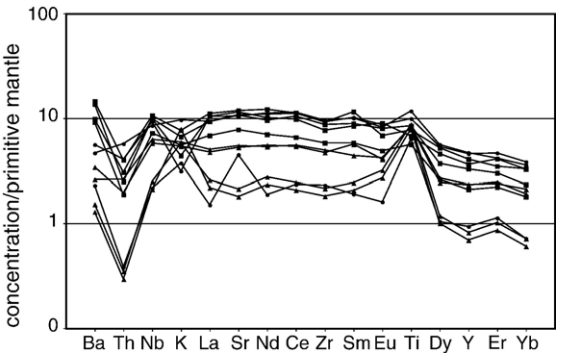

Fig. 8. Average trace element compositions (courtesy of A.V. Sobolev) for primitive East Greenland melts (from Table 7). All compositions corrected for the amount of olivine added or subtracted to obtain equilibrium with likely mantle olivine (see text for calculation method and rationale) and normalised according to McDonough and Sun (1995). Circles: Lower Basalts, squares: Milne Land Formation and triangles: Geikie Plateau Formation time-equivalent. The compositions divide into: (a) trace element-rich group A including two Lower Basalt and three Milne Land Formation compositions; (b) trace element-poor group B including one wall rock reaction product from the Lower Basalts and two compositions from the Geikie Plateau Formation time-equivalent; and (c) three intermediate group C compositions including one wall rock reaction product from Milne Land Formation and two compositions from the Geikie Plateau Formation time-equivalent.

three from the Milne Land Formation. The major element compositions are picritic with Mg#'s between 0.729 and 0.759 and with 2.33 to 1.29 wt.% TiO_2. They show a steady increase from Yb to Sr followed by a decrease to K, a Nb peak caused by lows in Th and K (Table 7, columns 1, 4, 5, 6 and 8).

(b) Group B compositions are low in trace element concentrations and includes one inclusion from the Lower Basalts and two from the Geikie Plateau Formation time-equivalent. They are generally lower in TiO_2 (1.16–1.60 wt.%) than group A, but rich in FeO(total) (14.94–17.11 wt.%) and with Mg#'s between 0.677 and 0.745 (Table 7, columns 3, 10 and 13). They have more or less developed peaks at K, Sr and TiO_2. They are all suggested to be products from wall rock cumulates or trace element-poor upper mantle cumulates. It must be emphasised that, even though the absolute concentration of TiO_2 is low, these compositions have well-developed Ti-peaks (Fig. 8).

(c) Group C includes two compositions from the Milne Land Formation and one from the Geikie Plateau Formation time-equivalent dyke. They have Mg#'s between 0.714 and 0.718, TiO_2 concentrations between 0.88 and 1.63 wt.% and FeO (total) between 13.61 and 16.46 wt.%. They are broadly intermediate between the enriched group A and the wall rock products in group B. They show a rather smooth trace element spectra apart from a moderate Th-low and a well-developed Ti-peak. They are in trace element compositions intermediate between groups A and B.

5.4. Equilibration P and T for trapped melts

The primary melts equilibrate with possible mantle olivine at pressures from 0.8 to 14.8 kbar (Table 7). Despite the large uncertainty of the *P*-estimate, it is noted that the two compositions equilibrating at $P \leq 6$ kbar are wall rock reaction products. Out of the remaining 11 compositions are 9 high *P* melts (>10 kbar) with pressures up to 14.8 kbar. The temperatures of equilibration for the high *P* melts vary between 1458 and 1522 °C. The last two compositions (361026/1–3 and 404017/1–4) equilibrated at a pressure of ca. 8 kbar and at temperatures of 1424–1434 °C. The *P* and *T* estimates for the melts with $P > 10$ kbar are comparable to those suggested for the West Greenland picrites (Table 6 in Larsen and Pedersen, 2000), and suggest that the present *P*-estimates can be used for a first order identification of melts trapped in olivine en route to the surface and melts trapped in the feeder chambers. The feeder chambers would be located at or near the base of the 35–41 km (11–14 kbar) thick crust in the Kangerlussuaq area (Trine Dahl-Jensen, pers. com., 2006). Picrite melts are supposed to have pooled in the feeder chambers before their ascent to surface.

5.5. Depth of segregation and initial melting.

The segregation depth in the mantle can be estimated from the CaO/Al_2O_3 ratio (Herzberg and Zhang, 1996). The CaO/Al_2O_3 ratio is independent of the remodelling of the primary composition, whereas the Al_2O_3 concentration is not. The modelled compositions, except the wall rock product, fall close to or slightly below the defined compositions for solidus melts and in the field of allowed melts (Fig. 9). This suggests that the modelled primary composition have been diluted with reasonable proportions of olivine. The depth of segregation varies from 2.8 to 4.7 GPa with most compositions between 3 and 4 GPa. A pressure of 3–4 GPa is equivalent to a depth of 90–120 km and is here suggested to be the depth of the boundary between the astenopheric and lithospheric mantle. The modelled compositions overlap in part with Hawaiian compositions (Fig. 9), but with a tendency for slightly higher pressures in accordance with the increasing depth of segregation with increasing age (Herzberg, 1995).

A very approximate estimate of the pressure for the initial melting can according to Herzberg and O'Hara (1998, Fig. 14) be obtained from the Al_2O_3 versus SiO_2 contents of the primitive melts (Fig. 10). It is observed that the compositions of melts of the Lower Basalts and the Milne Land Formation (columns 1–8 in Table 7) all,

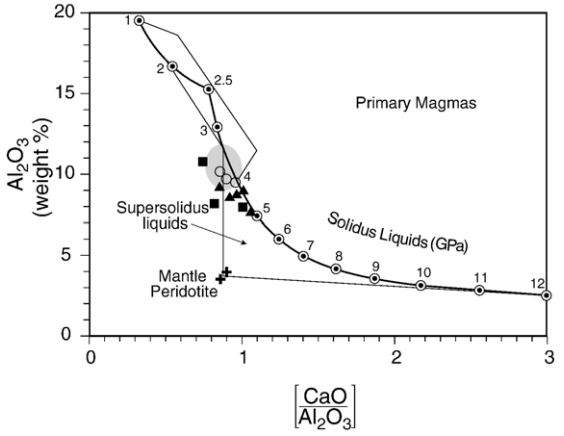

Fig. 9. Estimates of pressures of segregation based on Al_2O_3 versus CaO/Al_2O_3, after Herzberg and Zhang (1996). Symbols as in Fig. 7. Grey field: Hawaiian compositions (Herzberg, 1995).

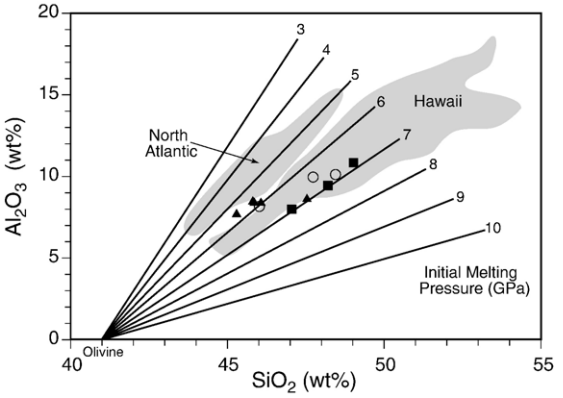

Fig. 10. Approximation to pressures of initial melting on basis of SiO_2 and Al_2O_3 contents after Herzberg and O'Hara (1998). The lines from the olivine composition (Fo92.3) give the approximate pressure of initial melting (GPa). Symbols as in Fig. 7. Solid line encircles Hawaiian compositions and stippled line North Atlantic compositions from West Greenland, the SE Greenland margin and Reykjaness, Iceland. Compositional fields after Herzberg and O'Hara (1998).

apart from one, have Al_2O_3/SiO_2 ratios in common with Hawaiian compositions. Pressures between 6 and 7 GPa are suggested, but as noted by Herzberg and O'Hara (1998), these pressures may be too high due to high Na_2O contents and the true pressures of initial melting would most likely be between 5 and 6 GPa. Nevertheless, Fig. 10 shows the similarity between the East Greenland and Hawaiian melts (except one).

The melts of Geikie Plateau formation time-equivalent are different. They have, except for one, lower Al_2O_3/SiO_2 ratios more in line with North Atlantic compositions from West Greenland, the SE Greenland shelf and Iceland (Fig. 10). Following Herzberg and O'Hara (1998), the difference may reflect variation in the contributions from recycled basaltic material, high in the early Lower Basalts and Milne Land Formation lavas and lower in the initial melts of the Geikie Plateau Formation time-equivalent. The change in the Al_2O_3/SiO_2 ratio could also be seen as the result of the developing and widening plume with an increasing core of residual harzburgite (see Herzberg and O'Hara, 1998, Fig. 4b and c) and progressing depletion of the source in response to the production of large volumes of plateau basalt melts.

6. Discussion

As stated in the introduction, the aim of this modelling is a search for the primary and enriched melts of the proto-Iceland plume in the Palaeogene magmatism in East Greenland. The compositional variations in the three formations (Fig. 2A–C) show that high TiO_2 as well as low-TiO_2 melts were available in all three stages of the evolution. Bulk sample may represent mixtures of components from different source rocks.

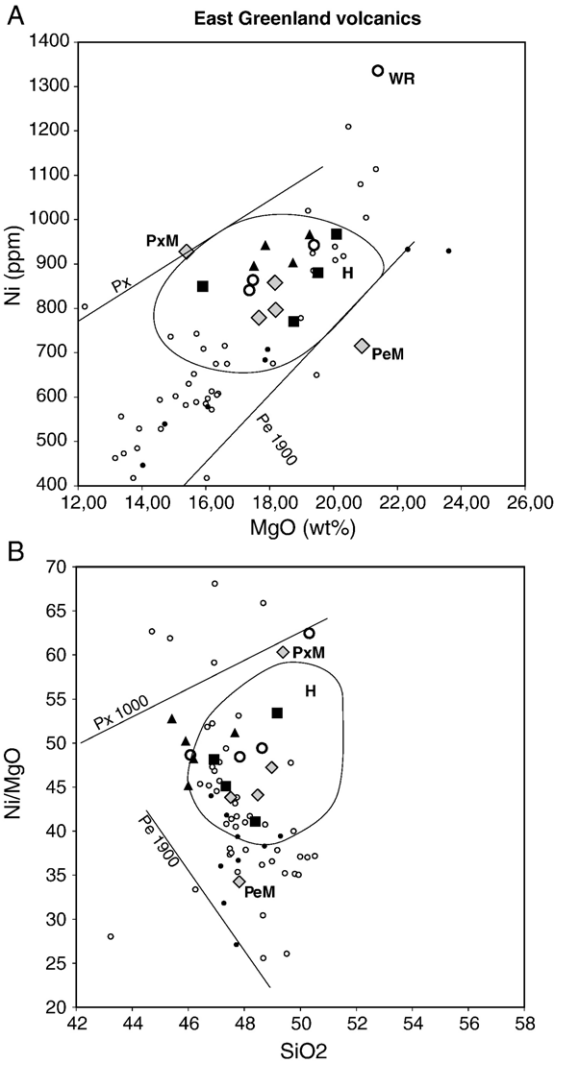

Fig. 11. Comparison between East Greenland and Hawaiian primitive melts. After Sobolev et al. (2005). (A). Ni vs. MgO in melts and lavas. Melts from the Lower Basalts (large circles), the Milne Land Formation (filled squares) and the Geikie Plateau Formation time-equivalent (triangles) plot within the field of primitive Hawaiian melts (H; after Sobolev et al., 2005). Circle marked WR is the wall rock reaction product from the Lower Basalts. Small circles are Lower Basalts with >13 wt.% MgO. Hawaiian melts are marked with diamonds: PxM: pyroxenitic end-member melt and PeM: peridotitic end-member melt. The three diamonds in the centre of the Hawaiian field are the suggested primary melts for Mauna Loa, Kilauea and Mauna Kea in Sobolev et al. (2005). Px line: melts in equilibrium with pyroxenite with 1000 ppm Ni and Pe1900 line: melts in equilibrium with fertile mantle lherzolite (bulk Ni=1900 ppm) at 3–5 GPa. See Sobolev et al. (2005) for explanation. (B). Ni/MgO vs. SiO_2 in melts and lavas. Symbols as in (A).

The high MgO and TiO_2 picrite melts of the Lower Basalts were by Nielsen et al. (1981) compared to Hawaiian picrites. The comparison was solely based on the petrography and the major element compositions. As shown in Fig. 11A and B, all the primary East Greenland compositions (Table 7), fall with few exceptions in the fields of primary Hawaiian melts as defined in Sobolev et al. (2005). Exceptions are the wall rock reaction product from the Lower Basalts and melts from the Geikie Plateau Formation time-equivalent. A Lower Basalts picrite composition straddles the boundary of the Hawaiian field. Too much olivine may have been added to this composition during equilibration between melt and host olivine (Table 4a). The major element similarities between the East Greenland (this work) and the Hawaiian melts (Herzberg and O'Hara, 2002; Sobolev et al., 2005) are further brought out in Table 8. The East Greenland and Hawaii compositions give very similar estimates of P and T and the modelled compositions of liquidus olivines.

The average of the five East Greenland composition with high trace element concentrations (group A) are in Fig. 12 plotted together with the averages of primary Kilauea and Mauna Loa melts (Sobolev et al., 2005), the averages for the East Greenland low concentration wall rock products (group B) and the average for the group C (intermediate) melts. Group A is, apart from a K-low (volatilisation during analysis?) and a small Ti-peak, bracketed by the average compositions for Mauna Loa and Kilauea primary melts (Sobolev et al., 2005),

Table 8
Comparison between primitive magmas from East Greenland and Hawaii

	E. Greenland	Hawaii	Hawaii	Hawaii	E. Greenland	Hawaii	E. Greenland
	This study	Herzberg and O'Hara	Sobolev et al.	Sobolev et al.	This study	Sobolev et al.	This study
	Lower Basalts	Kilauea 3F, APFM	Kilauea average	Mauna Kea average	Milne Land Fm.	Mauna Loa average	Geikie Plateau Fm.
P (kbar)[a]	11.6	11	14.6	11.6	10.1	10.0	11.8
T (°C)[a]	1470.5	1451.7	1497.4	1468.7	1468.3	1466.9	1481.4
T (°C)[b], comparison		1442.6	1450.7	1435.4		1458.0	
Error on T (°C)		9.1	46.7	33.3		8.9	
Equilibrium olivine[a]	89.4	89.8	90.4	90.3	89.3	90.8	87.3
Ol, comparison[c]		89.8	90.4	90.3		90.8	
Major elements (wt.%)							
SiO_2	47.41	48.00	47.64	48.55	48.09	49.04	46.20
TiO_2	2.15	2.05	1.91	1.81	1.48	1.51	1.55
Al_2O_3	9.37	10.50	9.57	10.15	9.44	10.25	8.42
Cr_2O_3	0.15	n.d.	n.d.	n.d.	0.21	n.d.	0.09
Fe_2O_3	1.27	1.62	1.15	1.09	1.50	1.27	1.57
FeO	11.30	10.10	10.12	9.95	11.23	9.60	13.76
MnO	0.22	0.18	0.00	0.00	0.20	n.d.	0.21
MgO	18.03	16.80	18.23	17.69	17.97	18.19	18.16
NiO	0.11	n.d.	0.00	0.10	0.11	0.11	0.12
CaO	8.41	8.60	9.27	8.64	7.68	8.04	8.29
Na_2O	1.40	1.78	1.61	1.61	1.92	1.71	1.49
K_2O	0.18	0.37	0.30	0.30	0.18	0.20	0.15
P_2O_5	0.00	0.00	0.20	0.20	0.00	0.20	0.00
Total	100.00	100.00	100.00	100.00	100.01	100.00	100.01
Mg#	0.740	0.748	0.762	0.760	0.763	0.772	0.700
Ni (ppm)	891	n.d.	797	779	838	858	917
Log fO_2[a]	−4.74	−4.33	−4.65	−4.87	−4.59	−4.49	−4.86
FeO(total)	12.45	11.56	11.16	10.94	12.58	10.74	15.17
CaO/Al_2O_3	0.901	0.819	0.968	0.851	0.825	0.784	0.986
Segregation P (kbar)[a]	35	28	40	32	30	25	42

n.d.: no data.

[a] Calculated in accordance with Larsen and Pedersen (2000) with K_D determined following Herzberg and O'Hara (2002). See text for explanation.

[b] T from Herzberg and O'Hara (2002) and Sobolev et al. (2005) obtained by interpolation to here given pressure assuming a gradient of 46 °C/GPa.

[c] Olivine compositions from Herzberg and O'Hara (2002) and Sobolev et al. (2005).

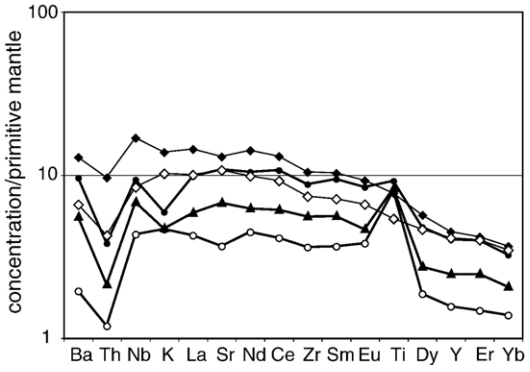

Fig. 12. Comparison between averaged trace element composition of East Greenland melts (Fig. 7) and Hawaiian melts (Sobolev et al., 2005). Filled diamonds: average Kilauea primitive melt and open diamond: average Mauna Loa primitive melts. The Hawaiian data is copied from Fig. S1 in Sobolev et al. (2005) and corrected for differences between normalisation factors. East Greenland: filled circle: average for "Hawaiian" type melts (group A, Fig. 8), open circle: average of low trace element compositions (group B, Fig. 8), and triangles: average of intermediate concentration melts (group C, Fig. 8). Note that the trace element-rich average is bracketed by the Hawaiian compositions. See text for discussion of deviations.

whereas the average for group B wall rock and group C melts have concentrations below the Hawaiian compositions. It is suggested that the group A melts from the earliest East Greenland lavas are equivalent to the primary melts from Hawaii. Following Sobolev et al. (2005), it is also suggested that the plume source for the melts was enriched in an eclogitic (recycled basalt) component in agreement with Korenaga and Kelemen (2000).

The pressure estimates suggest that melting was initiated at 5–6 GPa, that segregation of melt occurred at 3–4 GPa and that melts were mixed and started to crystallise in magma chambers at 10–15 kbar. The latter pressure appears to correlate with density trap below the East Greenland crust and the 3–4 GPa segregation pressure is suggested to correspond to the base of the lithospheric mantle. The envisaged scenario is that melting was initiated in the plume stem at depth of 150–180 km and that melting continued up through the plume structure and into the plume head at the base of the lithosphere. These melts are the Hawaiian type melts found in the melt inclusions. The melts subsequently separated from their source, mixed and rose to density trap magma at the base of the crust. The picrites dykes and lavas were tapped from the magma chambers at the base of the crust.

Inspired by Herzberg and O'Hara (1998, Fig. 4c), the Hawaiian type melts appear to characterise focussed plumes with limited proportions of harzburgitic residuals. In other words, plume that has not been extensively depleted in basaltic component. The size of the plume head below the East Greenland lithosphere is not known, but it seems likely that a high proportion of basaltic component in the Hawaiian type melts would suggest the melts to originate from near the plume stem. This questions the suggested passage of the stem of the Iceland plume under the present-day coast of East Greenland at 50 to 40 Ma (e.g., Lawver and Müller, 1994; Tegner et al., 1998b). The Hawaiian type melts from the stem of the focussed plume extruded between 61 and 57 Ma, and the plume stem was probably located beneath East Greenland at 57–61 Ma.

7. Conclusions

Despite all the uncertainties caused by reconnaissance nature of the study, the small number of studied samples, and the complexity of the equilibration and back-calculation, some of the early East Greenland melts appear to resemble primary Hawaiian melts. It seems to be a reasonable suggestion that the same types of sources and the same types of processes were responsible for the compositions of the primary melts in East Greenland (group A) and Hawaii. It is more than tempting to suggest that the initiation of the proto-Icelandic magmatism in East Greenland was strongly influenced by the impact of a "Hawaiian" type plume with a large component from recycled basaltic crust. The conclusions reached in this reconnaissance study are:

(1) The compilations of the bulk rock compositions from the Palaeogene of East Greenland and the data from the melt inclusions suggest many of the early lavas of the proto-Iceland plume lavas are mixtures of melts derived not only from different depth and different source rocks and that the compositions of primary melts varied over time.
(2) The earliest high MgO- and TiO_2-rich picrite compositions with elevated trace element concentrations (group A) compare to parental melts of the Hawaiian shield building stage and are suggested to show the rise of a more focussed "Hawaiian" type plume below East Greenland before the initiation of continental separation and seafloor spreading.
(3) An apparent change to more North Atlantic primary compositions as the large volume plateau basalts were extruded (Geikie Plateau Formation time) is suggested to signal the development of the proto-Iceland plume into a larger and more depleted plume responsible for the majority of the basalts in the North Atlantic province.

(4) The deep plume source contained a significant basaltic component in agreement with the conclusions of Korenaga and Kelemen (2000).
(5) The reconnaissance study shows that detailed information from the melt inclusions can add important new information on the early development of the Iceland plume.

Acknowlegements

All shown major element data on melt inclusion are copied from the final report of the INTAS-RFBR-95-953 project "Large igneous provinces: the role of ultramafic melts and volatiles", coordinated by C. Kent Brooks and Igor. D. Ryabchikov. All members of the INTAS-RFBR team are acknowledged for their contributions. INTAS and RFBR are gratefully acknowledged for the support for the studies of the melt inclusions. The average trace element data element was generously provided by A.V. Sobolev. The present work could not have been completed without the interest and support of C.K. Brooks, A.V. Sobolev, Lotte M. Larsen and S. Bernstein, and excellent reviews by Peter Kelemen, Andrey Gurenko and Christian Tegner.

Appendix A. Supplementary data

Supplementary data associated with this article can be found, in the online version, at doi:10.1016/j.lithos.2006.03.038.

References

Albarède, F., 1992. How deep do common basaltic magmas form and fractionate? Journal of Geophysical Research 97B, 10997–11009.
Andreasen, R., Peate, D.W., Brooks, C.K., 2004. Magma plumbing systems in large igneous provinces: inferences from cyclical variations in Palaeogene East Greenland basalts. Contributions to Mineralogy and Petrology 147, 438–452.
Brooks, C.K., 1973. Rifting and doming in southern East Greenland. Nature, Physical Sciences 244, 23–25.
Brooks, C.K., 1976. The Fe_2O_3/FeO ratio of basalt analyses: an appeal for a standardized procedure. Bulletin of the Geological Society of Denmark 25, 117–120.
Brooks, C.K., Nielsen, T.F.D., 1978. Early stages in the differentiation of the Skærgård magma, as revealed by a closely-related suite of dike-rocks. Lithos 11, 1–14.
Brooks, C.K., Nielsen, T.F.D., 1982. The E Greenland continental margin: a transition between oceanic and continental magmatism. Journal of the Geological Society (London) 139, 265–275.
Brooks, C.K., Ryabchikov, I.D., 1998. Large igneous provinces: the role of ultramafic melts and volatiles. Unpublished report: INTAS-RFBR-95-953. 226 pp.
Danyushevsky, L.V., Della-Pasqua, F.N., Sokolov, S., 2000. Re-equilibration of melt inclusions trapped by magnesian olivine phenocrysts from subduction-related magmas: petrological implications. Contributions to Mineralogy and Petrology 138, 68–83.
Danyushevsky, L.V., Leslier, R.A., Crawford, A.J., Durance, P., 2004. Melt inclusions in primitive olivine phenocrysts: the role of localized reaction processes in the origin of anomalous compositions. Journal of Petrology 45 (12), 2531–2553.
Ford, C.E., Russel, D.G., Craven, J.A., Fisk, M.R., 1983. Olivine-liquid equilibria: temperature, pressure and composition dependence of the crystal/liquid cation partition coefficients for Mg, Fe^{2+}, Ca and Mn. Journal of Petrology 24, 256–265.
Fram, M., Lesher, C.E., 1997. Generation and polybaric differentiation of East Greenland Early Tertiary flood basalts. Journal of Petrology 38, 231–275.
Gurenko, A.A., Chaussidon, M., 1995. Enriched and depleted primitive melts included in olivine from Icelandic tholeiite; origin by continuous melting of a single magma column. Geochimica et Cosmochimica Acta 59, 2905–2917.
Gurenko, A.A., Hansteen, T.H., Schmincke, H.-U., 1996. Evolution of parental magmas in olivine from Miocene shield basalts of Cran Canaria (Canary Islands): constraints from crystal melt and fluid inclusions in minerals. Contributions to Mineralogy and Petrology 124, 422–435.
Hansen, H., 1993. Tertiære basalter på Østgrønland. MSc Thesis, University of Copenhagen. App. II, Tabel AII-1, 2–5.
Hansen, H., Nielsen, T.F.D., 1999. Crustal contamination in Palaeogene East Greenland flood basalts: plumbing system evolution during continental rifting. Chemical Geology 157, 89–118.
Herzberg, C., 1995. Generation of plume magmas through time: an experimental perspective. Chemical Geology 126, 1–16.
Herzberg, C., O'Hara, M.J., 1998. Phase equilibrium constraints on the origin of basalts, picrites and komatiites. Earth-Science Reviews 44, 39–79.
Herzberg, C., O'Hara, M.J., 2002. Plume-associated ultramafic magmas of Phanerozoic age. Journal of Petrology 43 (10), 1857–1883.
Herzberg, C., Zhang, J., 1996. Melting experiments on anhydrous peridotite KLB-1: compositions of magmas in the upper mantle and transitional zone. Journal of Geophysical Research 101 (B4), 8271–8295.
Holm, P.M., 1988. Nd, Sr, Pb isotope geochemistry of the lower lavas, E Greenland Tertiary igneous province. In: Morton, A.C., Parson, L.M. (Eds.), Early Tertiary Volcanism and the Opening of the NE Atlantic. Geological Society Special Publication, vol. 39, pp. 181–195.
Kamenetsky, V.S., Eggins, S.M., Crawford, A.J., Green, D.H., Gasparon, M., Falloon, T.J., 1998. Calcic melt inclusions in primitive olivine at 43°N MAR: evidence for melt-rock reaction/melting involving clinopyroxene-rich lithologies during MORB generation. Earth and Planetary Science Letters 160, 115–132.
Kent, A.J.R., Baker, J.A., Wiedenbeck, M., 2002. Contamination and melt aggregation processes in continental flood basalts: constraints from melt inclusions in Oligocene basalts from Yemen. Earth and Planetary Science Letters 202, 577–594.
Kilinc, A., Carmichael, I.S.E., Rivers, M.L., Sack, R.O., 1983. The ferric–ferrous ratio of natural liquids equilibrated in air. Contributions to Mineralogy and Petrology 83, 136–140.
Korenaga, J., Kelemen, P.B., 2000. Major element heterogeneity in the mantle source of the North Atlantic igneous province. Earth and Planetary Science Letters 184, 251–268.
Kuno, H., 1969. Mafic and ultramafic nodules in basaltic rocks of Hawaii. Memoir-Geological Society of America 115, 189–234.

Larsen, L.M., Pedersen, A.K., 2000. Processes in high-Mg, high-T magmas: evidence from olivine, chromite and glass in Palaeogene picrites from West Greenland. Journal of Petrology 41 (7), 1071–1098.

Larsen, L.M., Watt, W.S., Watt, M., 1989. Geology and petrology of the Lower Tertiary plateau basalts of the Svcoresby Sund region, East Greenland. Bulletin-Grùnlands Geologiske Undersùgelse 157. 164 pp.

Larsen, M., Hamberg, L., Olaussen, S., Nørgaard-Pedersen, N., Stemmerik, L., 1999. Basin evolution in southern East Greenland: an outcrop analogue for Cretaceous–Palaeogene basins on the North Atlantic volcanic margins. Bulletin of the American Association of Petroleum Geologists 83 (8), 1236–1261.

Larsen, L.M., Pedersen, A.K., Sundvoll, B., Frei, R., 2003. Alkali picrites by melting of old metasomatized lithospheric mantle: Manîtdlat member, Vaigat Formation, Palaeocene of West Greenland. Journal of Petrology 44, 3–38.

Lawver, L.A., Müller, R.D., 1994. Iceland hotspot track. Geology 22, 311–314.

McDonough, W.F., Sun, S.-S., 1995. The composition of the Earth. Chemical Geology 120 (3&4), 223–253.

Nielsen, T.F.D., 1978. Dike swarms of the Kangerdlugssuaq Area, East Greenland and their bearing on the opening of the North Atlantic in Tertiary. Contributions to Mineralogy and Petrology 67, 63–78.

Nielsen, T.F.D., 2004. The shape and volume of the Skaergaard intrusion, Greenland: implications for mass balance and bulk composition. Journal of Petrology 45 (3), 507–530.

Nielsen, T.F.D., Soper, N.J., Brooks, C.K., Faller, C.K., Higgins, A.C., Matthews, D.W., 1981. The pre-basaltic lower basalts at Kangerdlugssuaq, East Greenland: their stratigraphy, lithology, palaeomagnetism and petrology. Meddelelser om Grønland. Geoscience 6 (25 pp.).

Peate, I.U., Larsen, M., Lesher, C.E., 2003. The transition from sedimentation to flood volcanism in the Kangerlussuaq basin, East Greenland: basaltic pyroclastic volcanism during initial Palaeogene continental break-up. Journal of the Geological Society (London) 160, 759–772.

Pedersen, A.K., Watt, M., Watt, W.S., Larsen, L.M., 1997. Structure and stratigraphy of the early Tertiary basalts of the Blosseville Kyst, East Greenland. Journal of the Geological Society (London) 154, 565–570.

Ramsay, R.R., Thompkins, L.A., 1994. The geology, heavy mineral concentrate mineralogy and diamond prospectivity of the Boa Esperanca and Cana Verde pipes, Córrega Dánta, Minas Gerais, Brazil. In: Meyer, H.O.A., Leonardos, O.H. (Eds.), Proceedings of the Fifth International Kimberlite Conference, Araxa, Brazil 1991. Vol. 2, Diamonds: Characterization, Genesis and Exploration. CPRM Special Publication 1/A, Brasilia, pp. 329–345.

Ryabchikov, I.D., Brooks, C.K., Kogarko, L.N., Nielsen, T., Solovova, I.P., Turkov, V., 1998. Tertiary picrites from Greenland: modelling sources and petrogenesis from melt inclusions. Mineralogical Magazine 62 (A), 1306–1307.

Sack, R.O., Carmichael, I.S.E., Rivers, M., Ghiorso, M.S., 1980. Ferric–ferrous equilibria in natural silicate liquids at 1 bar. Contributions to Mineralogy and Petrology 75, 369–376.

Sobolev, A.V., 1996. Melt inclusions in minerals as a source of principle petrological information. Petrology 4 (3), 228–239.

Sobolev, A.V., Nikogosian, I.K., 1994. Petrology of long-lived mantle plume magmatism: Hawaii, Pacific and Reunion Island, Indian Ocean. Petrology 2, 111–144.

Sobolev, A.V., Hofmann, A.W., Nikogosian, I.K., 2000. Recycled oceanic crust observed in “gost plagioclase” within the source of Mauna Loa lavas. Nature 404, 986–990.

Sobolev, A.V., Hofmann, A.W., Sobolev, S.V., Nikogosian, I.K., 2005. An olivine-free source of Hawaiian shield basalts. Naturen 434, 590–597.

Tegner, C., Lesher, C., Larsen, C.E., Watt, L.M., 1998a. Evidence from the rare-earth-element record of mantle melting for cooling of the Tertiary Iceland plume. Nature 395, 591–594.

Tegner, C., Duncan, R.A., Bernstein, S., Brooks, C.K., Bird, D.K., 1998b. ^{40}Ar–^{39}Ar geochronology of Tertiary mafic intrusions along the East Greenland rifted margin: relations flood basalts and the Iceland hotspot track. Earth and Planetary Science Letters 156, 75–88.

Turkov, V.A., Kogarko, L.N., Brooks, C.K., Nielsen, T.F.D., 1998. Comparison of the picrite evolution from East and West Greenland (melt inclusion data). Mineralogical Magazine 62 (A), 1549–1550.

Yaxley, G.M., Kamenetsky, V.S., Kamenetsky, M., Norman, M.D., Francis, D., 2004. Origins of compositional heterogeneity in olivine-hosted melt inclusions from the Baffin Island picrites. Contributions to Mineralogy and Petrology 148, 426–442.